

Molecular Stability and the
 $\text{H}_2 + \text{D}_2 \longrightarrow 2\text{HD}$ Four-Center
Exchange Reaction Surface

Thesis by
[Charles] Woodrow Wilson, Jr.

In Partial Fulfillment of the Requirements

For the Degree

Doctor of Philosophy

California Institute of Technology
Pasadena, California

1970

(Submitted April 6, 1970)

-i-

To my wife and my mother

... The most incomprehensible thing about the
universe is that it is comprehensible....

A. Einstein

T A B L E O F C O N T E N T S

Acknowledgements.....	iii
Introduction.....	1
The Nature of Chemical Forces	
A. Chemical Binding.....	3
B. Resonance.....	14
C. The Bond Region.....	21
D. Extrapolation to Larger Systems.....	31
The Reaction Surface for the $H_2 + D_2 \longrightarrow 2HD$	
Four-Center Exchange Reaction.....	39
A. The Shape of the Surface.....	40
B. Contragradience and the	
Energy Surface.....	43
Summary.....	53
References.....	55

A C K N O W L E D G E M E N T S

I would like to thank my wife Kathy for her sacrifices for my education, her existence has made the hard times easier. I thank her both for typing this thesis and for her many constructive criticisms of it.

I am especially indebted to my thesis advisor, Dr. William A. Goddard III; through countless hours of discussion he taught me to be a scientist. He allowed me to pursue my own interests, and took an active interest in whatever I was working on. I thank him especially for the questions he asked.

I am grateful to many of the Chemistry faculty, especially Dr. Aron Kuppermann, for their efforts on my behalf.

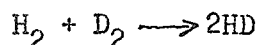
Members of other departments also worked on my behalf. Miss Kiku Matsumoto of the computer center staff donated many hours of her own time to assist me in programming. The tutoring of Miss Lolita Rosenstone of the Humanities Division was responsible for my passing the Ph.D. French requirement. I thank both of them.

I would also like to thank the entire secretarial staff of Noyes Laboratory, Mrs. Henriette Wymar, Mrs. Pat Anderson, and Miss Carol DeGroat, for many helpful discussions on the more standard orderings of letters, punctuation marks, and words in the English language.

Abstract

Partitions of the energy of the spin-coupling optimized GI wavefunctions of small systems are examined to isolate the factor responsible for chemical binding. One term, the contragradience energy, is found to dominate the binding energy in all cases. The magnitude of the contragradience energy is found to be insensitive to self-consistency effects; this property is used to extend the results to molecules too large for self-consistent calculation. Resonance, rotational barriers and the concept of a bond region are discussed in terms of the contragradience energy.

Calculations of the reaction surface for the



four-center exchange reaction are examined in terms of the contragradience energy.

I N T R O D U C T I O N

This thesis will examine trends common to mathematical models of a number of small systems of chemical interest to attempt to answer the questions of what the chemical bond is and why it occurs when it does. The concepts developed here will be applied to the energy hypersurface on which the



four-center exchange reaction occurs.

By examining these extremely small systems in detail, we hope to increase the understanding of the chemical behavior of far larger systems.

The most fundamental chemical properties of a system are characterized by chemical forces. While the large forces which stabilize atoms have been understood since the inception of quantum mechanics, the minor perturbation on these forces which stabilizes or destabilizes conglomerates of atoms is not yet well understood. It is the origin, nature, and sign of this perturbation, called chemical force, into which we shall delve first. We shall see that the chemical forces are as large as they are because the gradients of the bonding valence orbitals of constituent atoms are opposed throughout a region between the nuclei. (We will refer to the property of possessing opposed gradients as "contragradience"

throughout this thesis.)

For some time, chemists have found that many of their observations were consistent with the existence of a finite region, roughly between the nuclei, from which binding arises. Because the majority of the energy associated with the contragradience arises from a small region centered between the nuclei, we will be led quite naturally to the first theoretical definition of such a "bond region".

A study of the contragradience energy for rectangular H_4 will illustrate the applicability of these ideas to polyatomic systems and the conceptual simplifications which arise in using these concepts. It will also show the reason for the shape of the energy hypersurface and the height of the barrier to reaction in the



four-center exchange reaction.

Configuration interaction calculations over the region of the hypersurface which should contain the transition state complex for this reaction show the barrier height to be significantly above the dissociation energy of one of the reactant molecules. Thus it is quite likely that the reaction does not proceed by a four-center mechanism.

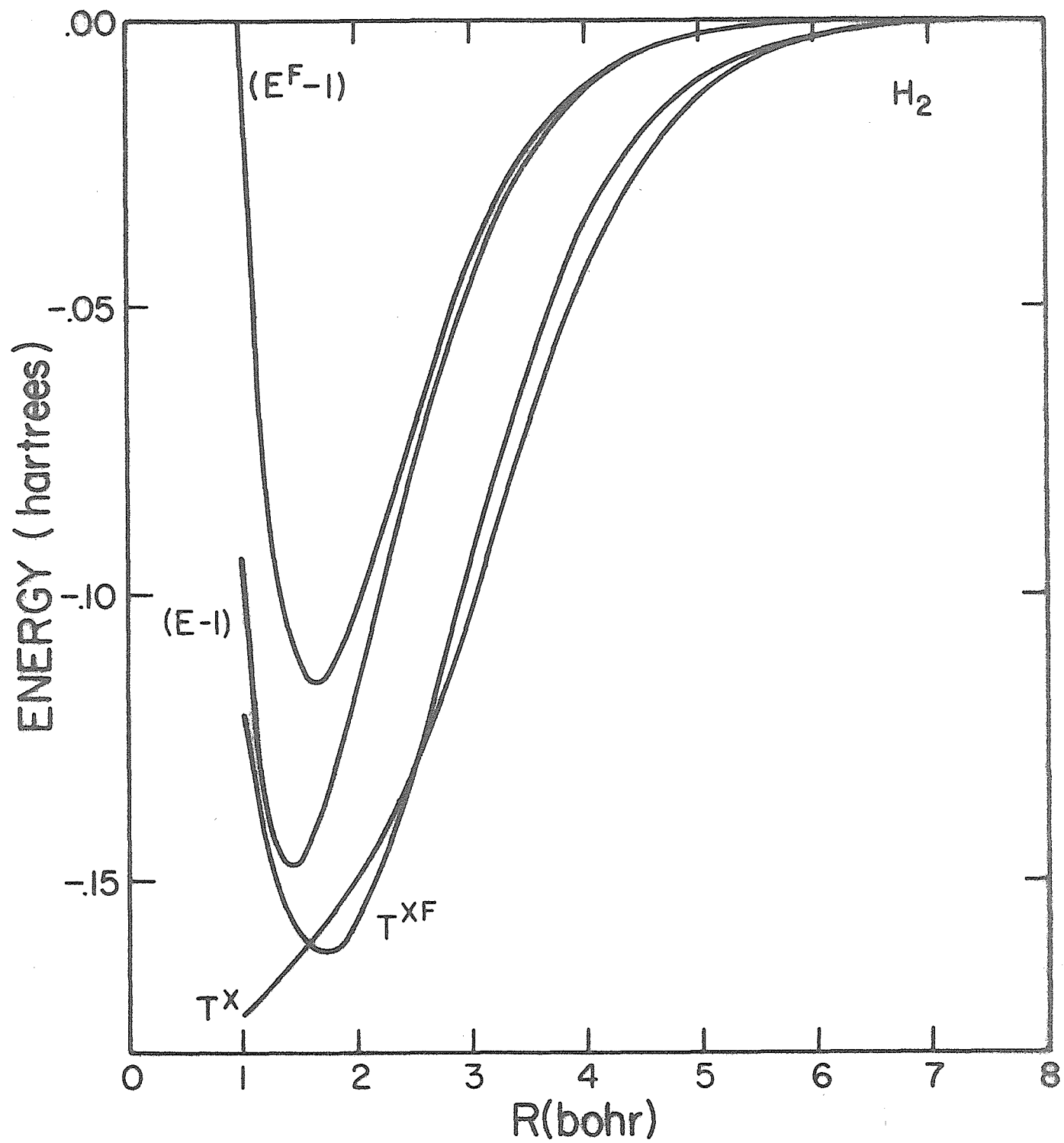
THE NATURE OF CHEMICAL FORCES

A. Chemical Binding

In their examination of the partitions of the energy of small chemical systems, Wilson and Goddard¹ have found that the binding energy of these systems closely parallels the change in one term in the energy expression: the nonclassical or exchange part of the kinetic energy, T^X . For example, the binding energy and ΔT^X for a self-consistent minimum basis set solution of the H_2 molecule are shown in Fig. 1 (note that the T^X curve must pass through the origin).

In the limit of large separation, the wavefunction of the molecule must asymptotically approach that of the dissociated species, in this case, two H atoms; therefore, at such separations we should be able to substitute the product of the wavefunctions of the dissociated species for the product of the self-consistent orbitals and achieve essentially the same results. Furthermore, empirically the tendency to bond is, at least in a zeroth order approximation, more strongly dependent on the nature of the constituent atoms than on that of the resultant molecule. Therefore,

Figure 1. The energy E and exchange kinetic energy T^X for the minimum basis set H_2 molecule. The curves labeled E^F and T^{XF} show the same quantities for the frozen solution.



we should expect that any term in the energy to which bonding may be attributed should not be highly dependent on the self-consistent solution for its magnitude. This suggests that we should freeze the wavefunction to be the properly anti-symmetrized product of the wavefunctions of the dissociated species. The energy E^F and exchange kinetic energy T^{XF} for this wavefunction are shown in Fig. 1, this shows us that the energy is highly dependent on self-consistency whereas T^X is not. Hence it is immediately apparent that, whatever is the effect responsible for the dominance of T^X , that effect is present in frozen wavefunction. Thus it will be sufficient to examine the frozen wavefunction in order to understand the dominance of T^X .

The GI wavefunction³ for the ground state of the H_2 molecule ($^1\Sigma g^+$) is

$$\Psi = G_1^{[2]} \phi_1 \phi_2 \alpha \beta = \frac{1}{2} (\phi_1 \phi_2 + \phi_2 \phi_1) (\alpha \beta - \beta \alpha)$$

where ϕ_1 and ϕ_2 are the one electron spatial functions and α and β are the spin functions. For the SCF solutions, these are functionally optimized, but here we will deal with them only as the simple atomic functions on each center. The classical, or Hartree, kinetic energy of this wavefunction is simply the sum of the one electron kinetic energies.

$$T^{\alpha} = t_{11} + t_{22}$$

where

$$t_{ij} = \langle \phi_i | -\frac{1}{2} \nabla^2 | \phi_j \rangle.$$

The rest of the kinetic energy is the nonclassical or exchange

contribution

$$\begin{aligned} T^X &= T - T^{CL} \\ &= -SD(t_{11} + t_{22} - \frac{2}{S} t_{12}) \end{aligned} \quad (1a)$$

where S is simply the overlap between orbitals 1 and 2,

$$S \equiv \langle \phi_1 | \phi_2 \rangle$$

and D is just the standard off-diagonal density matrix element.³

In this case it is given by

$$D = \frac{S}{1 + S^2}$$

Similarly the nonclassical part of the nuclear attraction can be written as

$$V^{nx} = -SD(v_{11}^n + v_{22}^n - \frac{2}{S} v_{12}^n)$$

where

$$v_{ij}^n = \langle \phi_i | v^n | \phi_j \rangle$$

and v^n is the nuclear attraction operator. Integrating by parts,

Eqn. (1a) can be rewritten as

$$T^X = -\frac{SD}{2} \left(\langle |\nabla \phi_1|^2 \rangle + \langle |\nabla \phi_2|^2 \rangle - \frac{2}{S} \langle \nabla \phi_1 \cdot \nabla \phi_2 \rangle \right) \quad (1b)$$

From Eqn. (1b), the distinction between T^X and the exchange part of the nuclear attraction energy V^{nx} is readily apparent: The third term, called the interchange term, is the expectation value of a vector dot product rather than of a simple scalar. This is unique within the energy expression! To evaluate the importance of this term, let us neglect the dot product nature of the term and replace the interchange term with the expectation value of the product of the magnitudes of the gradients, this leads to a new quantity

$$T^{nc} = -\frac{SD}{2} \left(\langle |\vec{\nabla} \phi_1|^2 \rangle + \langle |\vec{\nabla} \phi_2|^2 \rangle - 2 \langle |\vec{\nabla} \phi_1| |\vec{\nabla} \phi_2| \rangle \right) \quad (2)$$

which, for the frozen H_2 wavefunction, vanishes identically at all R!

This means that the drop in T^{XF} for the H_2 molecule is entirely due to the vector dot product within the interchange term! The difference between the product of the magnitudes and the dot product is simply

$$|\vec{\nabla} \phi_1| |\vec{\nabla} \phi_2| - \vec{\nabla} \phi_1 \cdot \vec{\nabla} \phi_2.$$

This is the quantity which is responsible for the existence of the chemical bond. The behavior of such an important quantity merits further examination. Our frozen orbitals are simple 1s hydrogenic orbitals, one centered on each nucleus; their gradients point radially outward from the nuclei at their respective centers. Proceeding along the internuclear axis, the quantity vanishes outside of the region between the nuclei. Passing through one of the nuclei, one of the gradients suddenly changes direction by 180° , leaving the two gradients opposed; the value of the quantity is quite large there. It remains constant until passing through the other nucleus whereupon it vanishes again. Because it depends on the gradients being opposed for its magnitude, we call this quantity the "contragradience function". We will designate the expectation value of this function between two orbitals as their contragradience.

From Eqns. (1b) and (2), we see that the contragradience contribution to the energy is simply

$$C = -D \langle \{ |\vec{\nabla} \phi_1| |\vec{\nabla} \phi_2| - \vec{\nabla} \phi_1 \cdot \vec{\nabla} \phi_2 \} \rangle$$

for the $^1\Sigma_g^+$ state of H_2 ,

$$C = -\frac{S}{1+S^2} \langle \{ |\nabla \phi_1| |\nabla \phi_2| - \nabla \phi_1 \cdot \nabla \phi_2 \} \rangle. \quad (3)$$

The first excited state of the H_2 molecule ($^3\Sigma_u^+$) also dissociates to two H atoms in their ground states. Let us examine this state to discover why it is not stable. The spin part of the singlet wavefunction is anti-symmetric (i.e. $\alpha\beta - \beta\alpha$) which forces the spatial part to be symmetric (i.e. $\phi_1\phi_2 + \phi_2\phi_1$). The situation is exactly reversed for the triplet state,

$$\Psi = G_1^{[2]} \phi_1 \phi_2 \alpha\beta = \frac{1}{2} (\phi_1 \phi_2 - \phi_2 \phi_1) (\alpha\beta + \beta\alpha).$$

For the anti-symmetrically coupled orbitals,

$$D = -\frac{S}{1-S^2}.$$

This leads to a contragradience energy of the form

$$C = \frac{S}{1-S^2} \langle \{ |\vec{\nabla} \phi_1| |\vec{\nabla} \phi_2| - \vec{\nabla} \phi_1 \cdot \vec{\nabla} \phi_2 \} \rangle. \quad (4)$$

Comparison of Eqns. (3) and (4) with the frozen case in mind shows that the contragradience is the same in both cases, making the contragradience energy dominant in both bonds. However, the substitution of an anti-symmetric spatial wavefunction for a symmetric one has changed the sign of the density matrix and hence has changed the sign of the contragradience energy; thus the contragradience energy makes a highly repulsive contribution to the binding energy and we would expect the $^3\Sigma_u^+$ state of H_2 to be unbound.

Allowing the frozen wavefunction to relax self-consistently, the energy is lowered. The ground state ($^1\Sigma_g^+$) is already strongly bound by the contragradience and the self-consistent orbitals retain

a strong resemblance to the frozen orbitals. They remain functions primarily localized on separate centers. This maintains the magnitude of their contragradience. The amplitude of the orbitals is increased in the region between the nuclei; this increases their overlap, decreasing C . In the triplet case ($^3\Sigma_u^+$) where C makes a highly repulsive contribution, self-consistency involves drastic changes in the orbitals, however even these drastic self-consistency effects will generally be insufficient to attain a bound state.

An examination of a number of chemical systems^{1b} both bound and unbound affirmed our conclusion that T^X , and therefore C , is the dominant term in the binding energy. (This examination included both the frozen and the self-consistent wavefunctions for the ground states of H_2 , H_2H , HeH , $(H_2)_2$, HeH_2 , He_2 , LiH , and BH .)

These partitions of the energy are exceptionally useful from a conceptual viewpoint because they can rigorously be expressed as a sum of pair interactions, thus

$$T^X = \sum_{i>j} -S_{ij} D_{ij}^i [t_{ii} + t_{jj} - \frac{2}{S_{ij}} t_{ij}]$$

and

$$C = \sum_{i>j} -D_j^i \langle \{ |\nabla\phi_i||\nabla\phi_j| - \nabla\phi_i \cdot \nabla\phi_j \} \rangle$$

where the sign of D_j^i is predictable from the spin coupling of the i^{th} and j^{th} electron. Thus we may speak of the contragradience energy of a pair of orbitals.

$$C_{ij} = -D_j^i \langle \{ |\nabla\phi_i||\nabla\phi_j| - \nabla\phi_i \cdot \nabla\phi_j \} \rangle \quad (5a)$$

and the total contragradience energy is simply the sum of the pair energies,

$$C = \sum_{i>j} C_{ij}. \quad (5b)$$

Equations (5) permit a straightforward discussion of systems with more than two electrons as a set of two electron problems. For more than two electrons, a discussion of the spin-coupling of the pairs is most simply accomplished in terms of the Young tableaux (see, for example Ref. 3). Here the spatial part of the two electron singlet is represented by the tableau

1	2
---	---

(when successive numbers occur in the same row, we may think of them as indicating a symmetric singlet pair of electrons). Two He atoms in their ground states at infinite separation have the tableaux

1	2
---	---

and

3	4
---	---

and lead to the combined tableau

1	2
3	4

for the system at finite separation. But C_{ij} is positive for i and j in different rows (think of this as i and j in different bonds). Thus all the interatomic interactions increase the energy, and hence He_2 should be unbound. On the other hand, the ground state of the LiH molecule is also described by the tableau

1	2
3	4

which arises from the atomic tableaux

1	2
3	

and

4

Here, the interatomic terms are C_{14} , C_{24} , and C_{34} . Orbitals 1 and 2 are core orbitals--which are concentrated near the nucleus and characteristically have a very low overlap with the H orbital--so their contributions to C , while positive, are small. The valence-valence term C_{34} dominates, and because it is negative the ground state of the LiH molecule should be bound.

From the dominance of the contragradience energy and its relative independence of self-consistency, we are led to a simple three-step model of the formation of the chemical bond:

1. We start with the orbitals which are appropriate for the infinitely separated atoms.
2. We bring the atoms to finite separation without allowing the orbitals to readjust. This leads to a large drop in the total energy due to the change in the contragradience energy, if the system is to be bound. A rise in the energy occurs for the same reason in systems which will not be bound.
3. Finally, a small decrease in the total energy is attained by allowing the orbitals to relax self-consistently.

This step makes the subtle changes in the wavefunction which allow it to satisfy the virial theorem, the Hellmann-Feynman theorem, etc.

It must be emphasized here that it is the second step, the bringing together of the frozen atoms, and not the third step, self-consistency, which is responsible for the occurrence of chemical

binding. Indeed, it is the relative independence of molecular stability from the third step which is primarily responsible for the success of the predictive schemes of chemistry, e.g., using the periodic table to predict chemical behavior.

B. Resonance

A consideration of the scheme which we have presented above immediately raises the question of the stability of H_2^+ ; it has only one electron, so it has no permutation symmetry, yet H_2^+ is bound.

In order to understand this stability, let us first consider a series of the singlet excited states of H_2 , those which dissociate to one H atom in its 1s level, and the other in its ns level.

Classically, at large separations, we can distinguish whether the excitation is on one atom or the other. If it is on say the right side, then we would have the corresponding quantum mechanical wavefunction

$$\Psi^R(1,2) = (\phi_{1s}^L(1)\phi_{ns}^R(2) + \phi_{ns}^R(1)\phi_{1s}^L(2)) / (a\beta - \beta a) \quad (6a)$$

or equivalently, for the excitation being on the left center

$$\Psi^L(1,2) = (\phi_{1s}^R(1)\phi_{ns}^L(2) + \phi_{ns}^L(1)\phi_{1s}^R(2)) / (a\beta - \beta a). \quad (6b)$$

Here we would expect to obtain some stabilization because of the spatial permutation symmetry. Quantum mechanically, the situations described by (6a) and (6b) are indistinguishable, adiabatically there is an equal probability of either situation. Thus the correct quantum mechanical states must be the symmetric and anti-symmetric combinations of (6a) and (6b). For the $^1 \Sigma_g^+$ states, for example

$$\Psi(1,2) = N (\Psi^R(1,2) + \Psi^L(1,2)), \quad (6c)$$

where N is a normalization constant. Now the classical kinetic energy is determined by the product wavefunction $\phi_{1s}^L \phi_{ns}^R$ or

$$\phi_{1s}^R \phi_{ns}^L,$$

$$T^{cl} = \langle \phi_{1s}^L | -\frac{1}{2} \nabla^2 | \phi_{1s}^L \rangle + \langle \phi_{ns}^R | -\frac{1}{2} \nabla^2 | \phi_{ns}^R \rangle$$

or

$$= \langle \phi_{1s}^R | -\frac{1}{2} \nabla^2 | \phi_{1s}^R \rangle + \langle \phi_{ns}^L | -\frac{1}{2} \nabla^2 | \phi_{ns}^L \rangle$$

which are equivalent. This leaves the nonclassical (or exchange)

kinetic energy which is composed of two terms in this case: the

term discussed previously, T^X ,

$$T^X = -\frac{S}{1+S} \left(\langle \phi_{1s}^L | -\frac{1}{2} \nabla^2 | \phi_{1s}^L \rangle + \langle \phi_{ns}^R | -\frac{1}{2} \nabla^2 | \phi_{ns}^R \rangle - \frac{2}{S} \langle \phi_{1s}^L | -\frac{1}{2} \nabla^2 | \phi_{ns}^R \rangle \right)$$

or

$$= -\frac{S}{1+S} \left(\langle \phi_{1s}^R | -\frac{1}{2} \nabla^2 | \phi_{1s}^R \rangle + \langle \phi_{ns}^L | -\frac{1}{2} \nabla^2 | \phi_{ns}^L \rangle - \frac{2}{S} \langle \phi_{1s}^R | -\frac{1}{2} \nabla^2 | \phi_{ns}^L \rangle \right)$$

where

$$S = \langle \phi_{1s}^L | \phi_{ns}^R \rangle = \langle \phi_{1s}^R | \phi_{ns}^L \rangle$$

and an additional term due to the exchange between the degenerate

configurations, \bar{T}^X

$$\bar{T}^X = \frac{\langle \psi^R | \psi^L \rangle}{2(\langle \psi^R | \psi^R + \psi^L \rangle)} \left(\langle \psi^R | -\frac{1}{2} \nabla^2 | \psi^R \rangle + \langle \psi^L | -\frac{1}{2} \nabla^2 | \psi^L \rangle - \frac{2 \langle \psi^R | -\frac{1}{2} \nabla^2 | \psi^L \rangle}{\langle \psi^R | \psi^L \rangle} \right).$$

In the limit as n becomes infinite in Eqns. (5), we obtain

the H_2 molecule ion, T^X vanishes, but \bar{T}^X remains to stabilize the

system. In Fig. 2, we show \bar{T}^X and E for frozen H_2^+ and we see that

the binding energy parallels the change in \bar{T}^X as we would have

expected.⁴ From the form of \bar{T}^X ,

$$\bar{T}^X = -\frac{S}{2(1+S)} (t_{11} + t_{22} - \frac{2}{S} t_{12}), \quad (7)$$

the reason for the continued dominance of the exchange kinetic

energy is obvious. Comparison of equations (1a) and (7) shows that

it is the contragradience between the orbitals comprising the two

Figure 2. The total energy E and exchange kinetic energy \bar{T}^X for minimum basis set H_2^+ . The results for the frozen and self-consistent solutions are shown. Although \bar{T}^{XF} is unique, there is some degree of arbitrariness in defining the SCF \bar{T}^X . (See Ref. 4.)

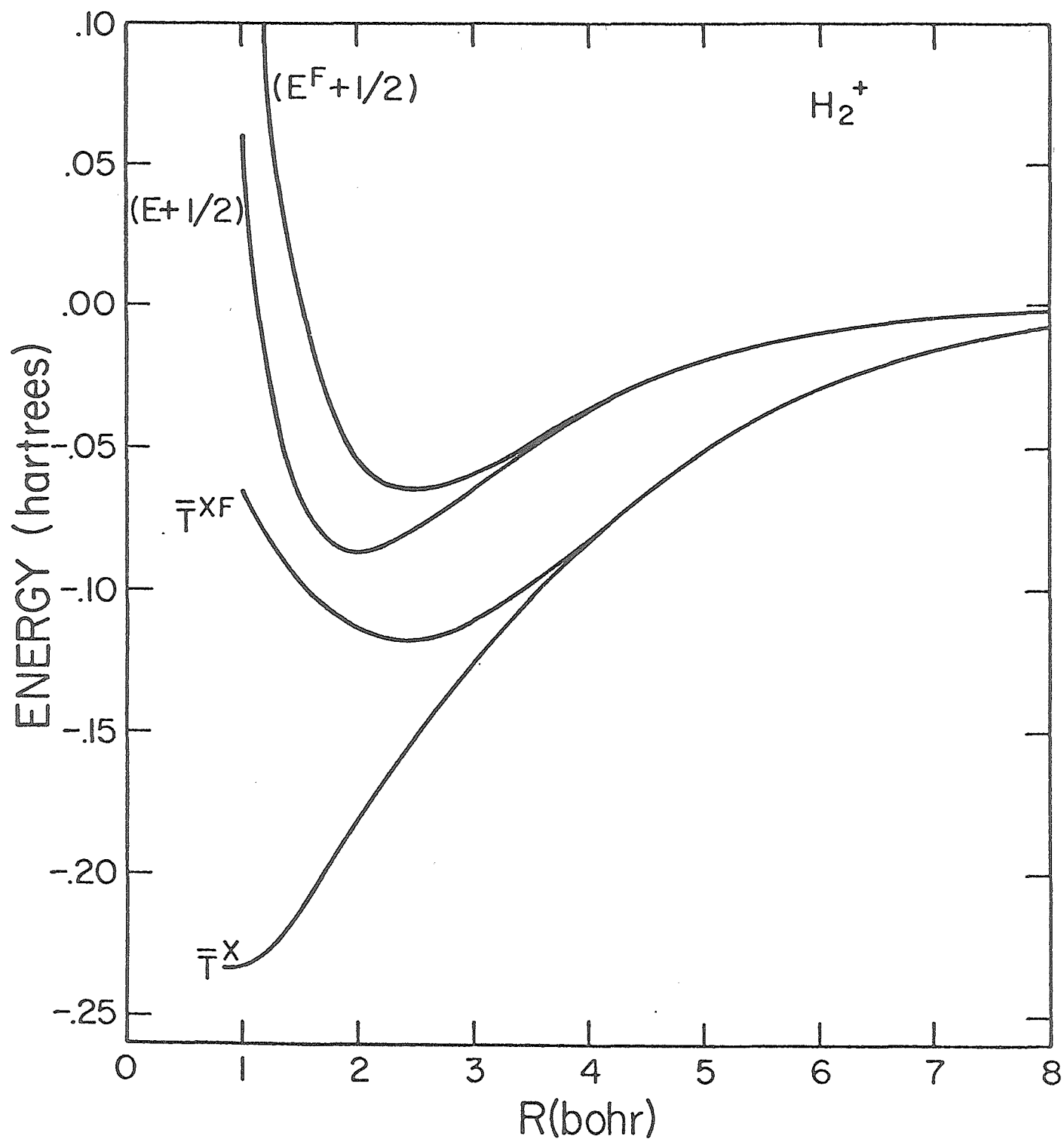
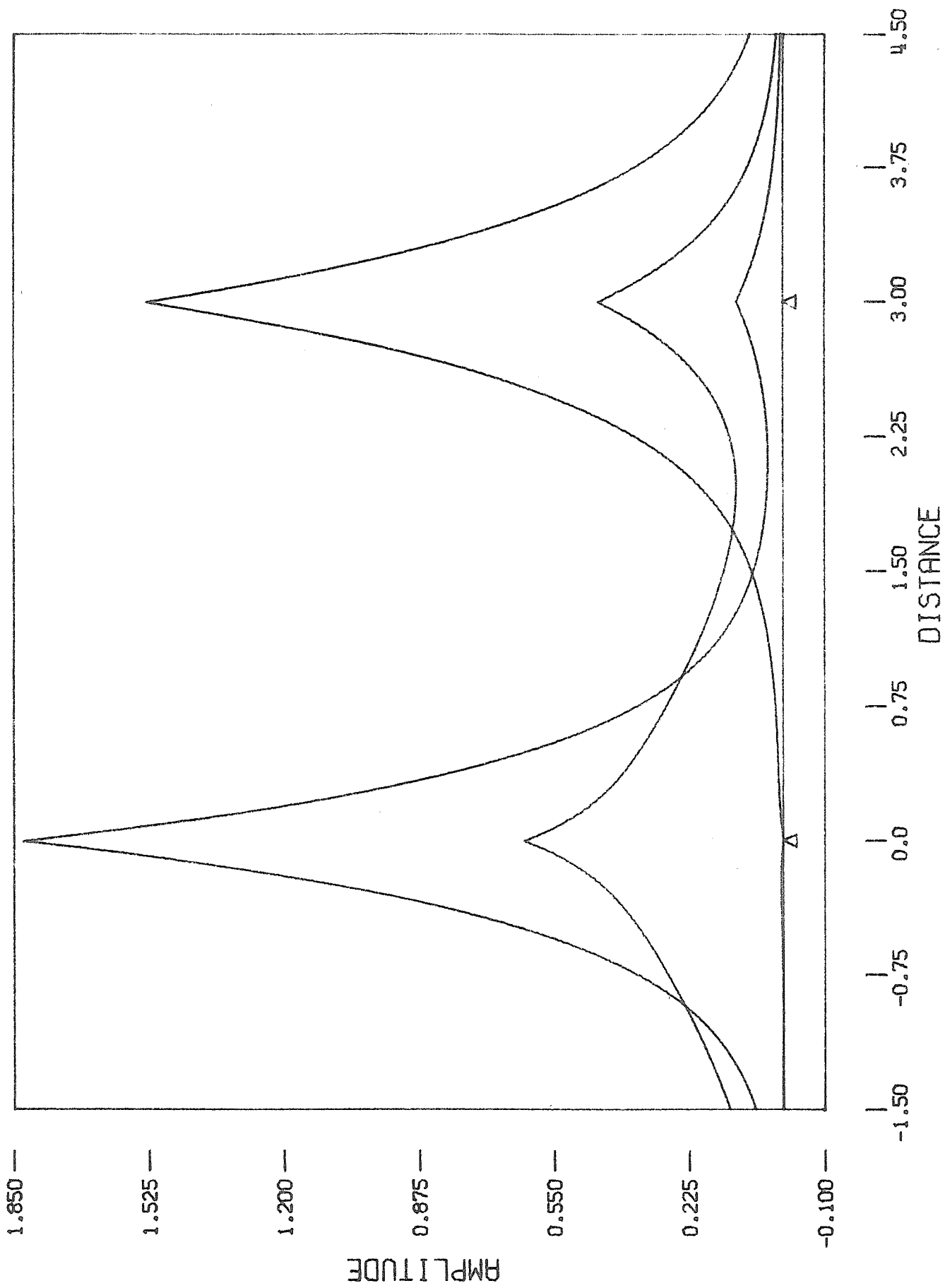


Fig 5

degenerate configurations which causes the bond to form.

In larger systems, e.g. the He_2^+ molecule-ion, the appropriate wavefunction is a two configuration extended CI wavefunction. The existence of the two degenerate configurations causes a large contribution from \bar{T}^X , producing a net change of -0.050 hartrees in the exchange kinetic energy for He_2^+ at a separation of 5.0 bohr. The binding energy is 0.040 hartrees at this separation. The self-consistent orbitals for one configuration are shown in Fig. 3. The significant lowering of energy caused by the mixing of degenerate or nearly degenerate configurations, which we have observed above, is the effect usually labeled as "resonance" by chemists. The important point here is that this energy lowering is again dominated by the exchange kinetic energy because of the contragradient nature of orbitals on different centers. Here again, the contragradience enters the energy expression by way of a nonclassical symmetry correction. Hence the useful concept of "resonance" is neither so significantly different from ordinary chemical bonding, nor so incomprehensible as it is sometimes made out to be.

Figure 3. The self-consistent orbitals for $^2\Sigma_u^+ \text{He}_2^+$ at $R = 3.0a_0$. These orbitals form one configuration of a two configuration extended GI wavefunction. The total wavefunction is the normalized anti-symmetric combination of this configuration and its mirror image.



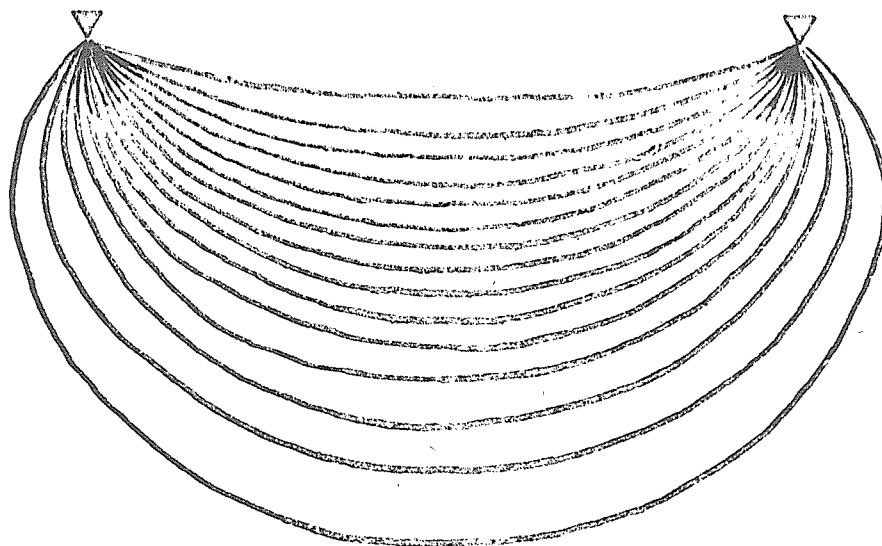
C. The Bond Region

Empirical observation of the properties of the chemical bond, e.g. the additivity of bond energies, have been interpreted as indicating that the bond arises from a small (but nebulous) region localized between the nuclei. In the above, we have seen that the two most important chemical forces, chemical bonding and resonance stabilization, arise from the contragradient nature of orbitals centered on different centers. The contragradient energy arises from those regions of space in which the gradients of the orbitals are large and antiparallel, or at least oblique; thus it arises predominately from a small volume centered between the nuclei. Since the contragradient energy arises primarily from this region, we may consider it as the bond region. We might, for example, define the bond region for the bond involving orbitals i and j as that region within a surface of constant contragradient c_{ij} contributing most (say 95%) of the contragradient energy C_{ij} .

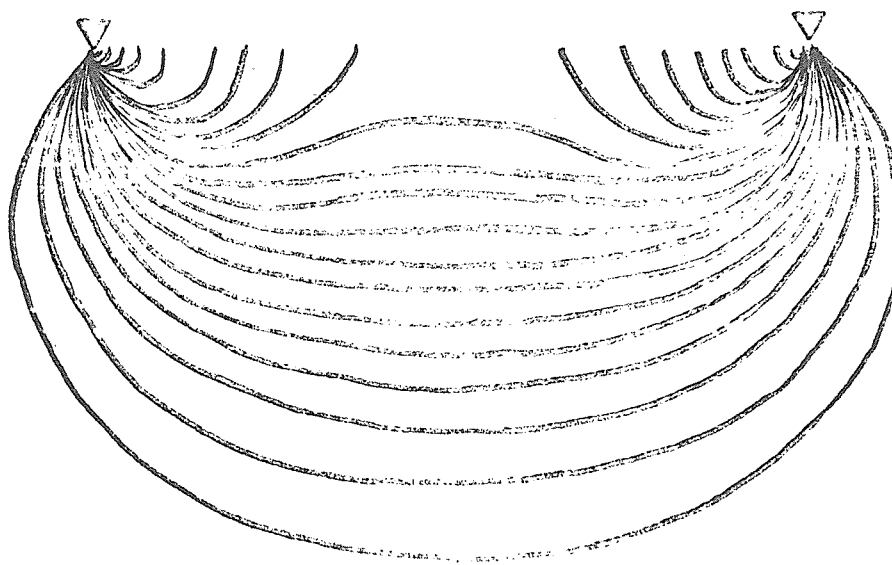
In Fig. 4, we show the integrand of contragradient energy for H_2 (see Eqn. 3) at the experimental equilibrium internuclear separation 1.4 bohr, for the frozen and self-consistent wavefunctions. In both cases, the region enclosed by the outer contour accounts for approximately 80% of the total contragradient energy. The shape and size of these regions are quite consistent with what one might expect the bond region to look like. Let us now examine

Figure 4. Contributions to the contragradience energy for the G1 wavefunction of H_2 at $R = 1.4$ bohr, (the contours are equally spaced with the outer contour being at $-.0045$ hartree/bohr³ with steps of $-.0045$ hartree/bohr³).

- A. Frozen wavefunction
- B. Self-consistent calculation with eight Slater-type basis functions.



A



B

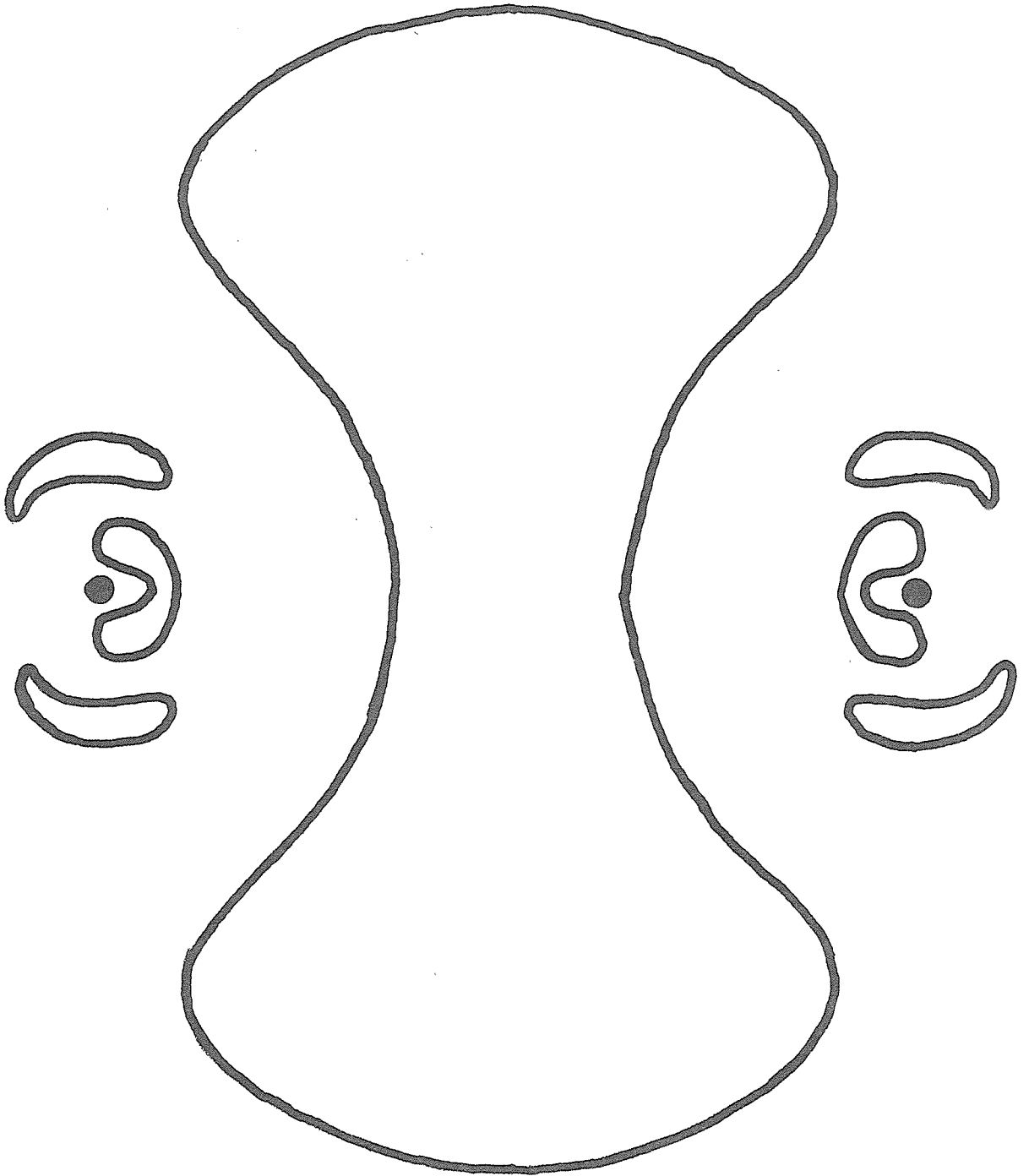
the bond regions in other systems of chemical interest. In Fig. 5, we show the bond region for the bond in the Li_2 molecule and for the bond in the LiH molecule; here we see that the bond region is localized between the nuclei and that the core region of the Li atom has been excluded. We see that the bond region near the Li atom has the same characteristic shape whether bonded to another Li atom or to an H atom. Comparison of Figs. 4 and 5b shows that the region near the H is also relatively insensitive to whether it is bonded to a Li atom or another H atom.

From a comparison of Figs. 4a and 4b, we see that the bond region, as defined above, is relatively insensitive to self-consistency; thus we may use frozen wavefunctions to map the bond regions of molecules even if self-consistent wavefunctions are not available, or are impractical. As another example we show in Fig. 6 the π -bond regions for ethylene, ($\text{H}_2\text{C}=\text{CH}_2$). The results are again entirely consistent with empirically based concepts of the bond region: two regions arrayed above and below the inter-nuclear axis, but close to it.

Thus we see that the concept of contragradience leads not only to an explanation of the existence and strength of the chemical bond and of resonance stabilization, but also to a natural definition of the bond region. The shape, location, and general behavior of the bond region as defined above is consistent with empirical discussions of this region.

Figure 5. Contributions to the contragradience energy for Li
containing bonds at equilibrium separation. (The contour
spacing is linear.)

- A. The G1 wavefunction for Li_2 .^{5a}
- B. The G1 wavefunction for LiH .^{5b}



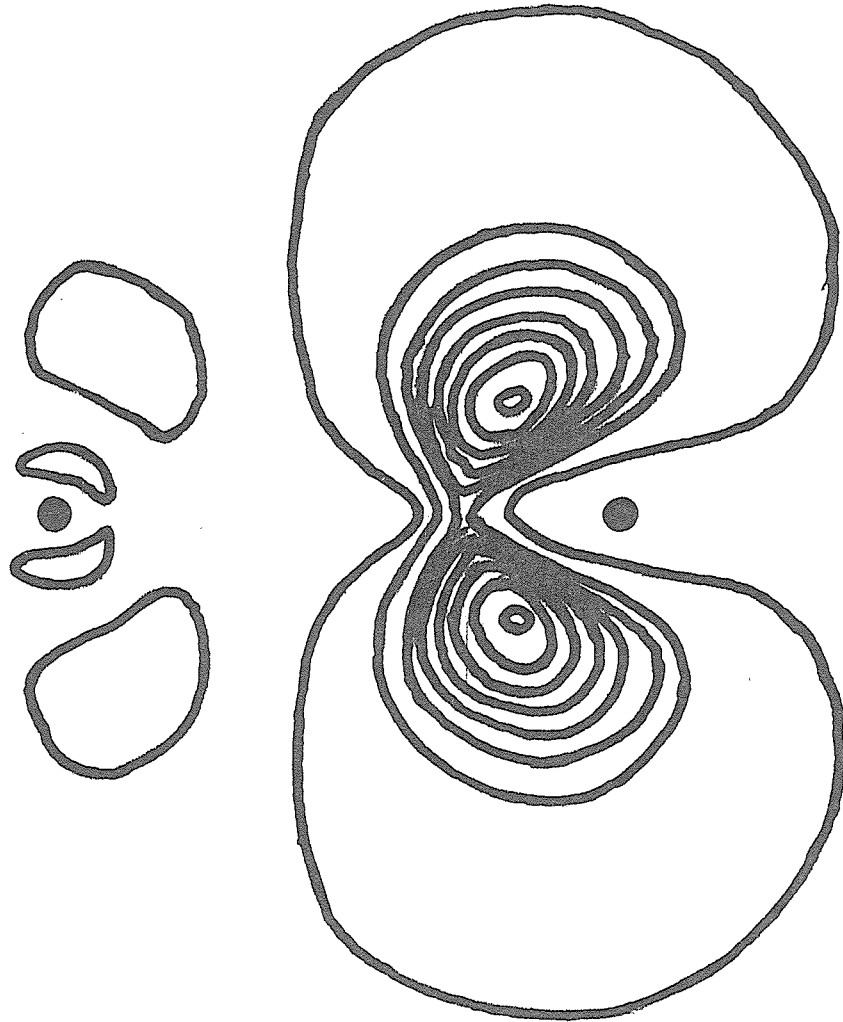
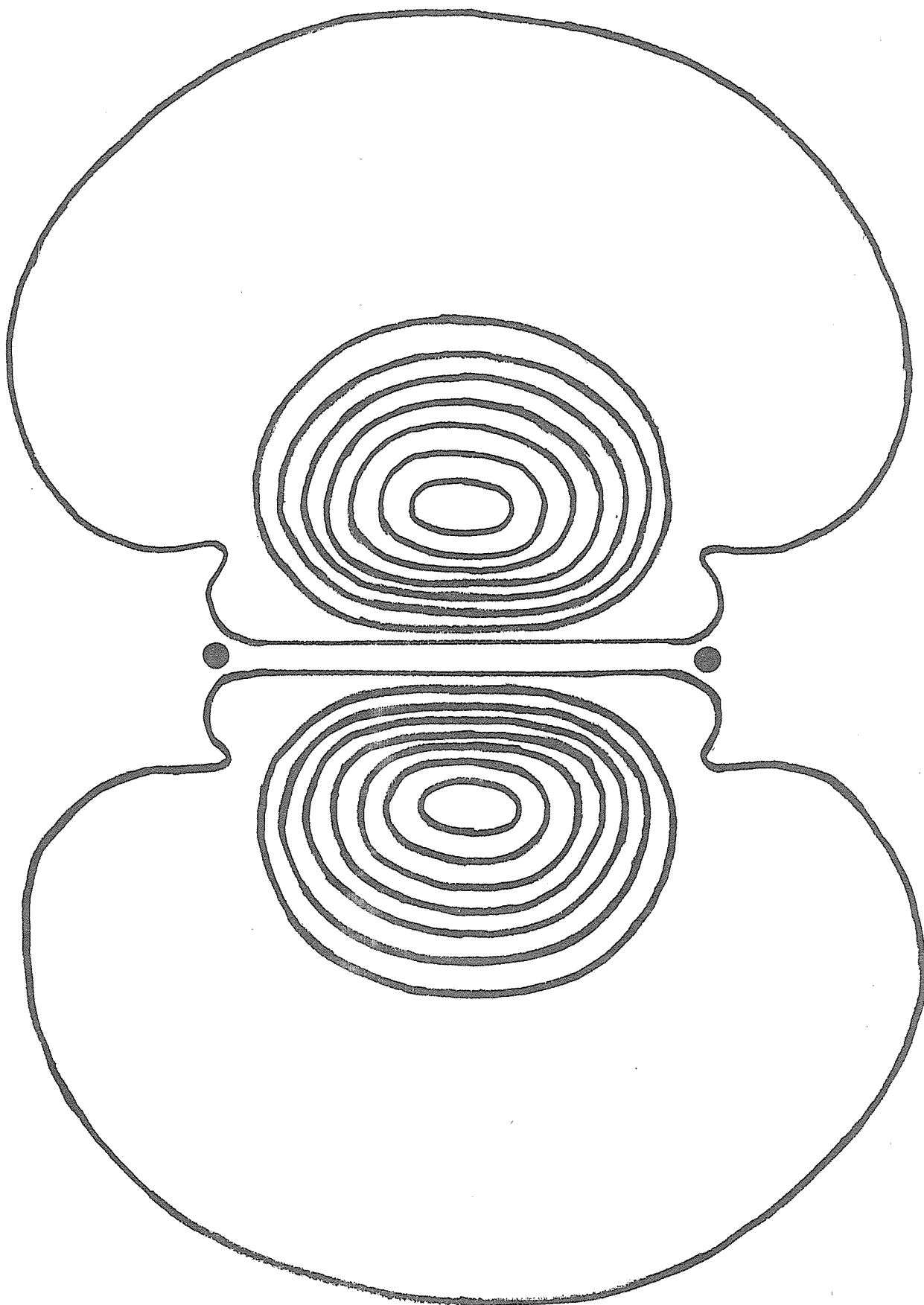
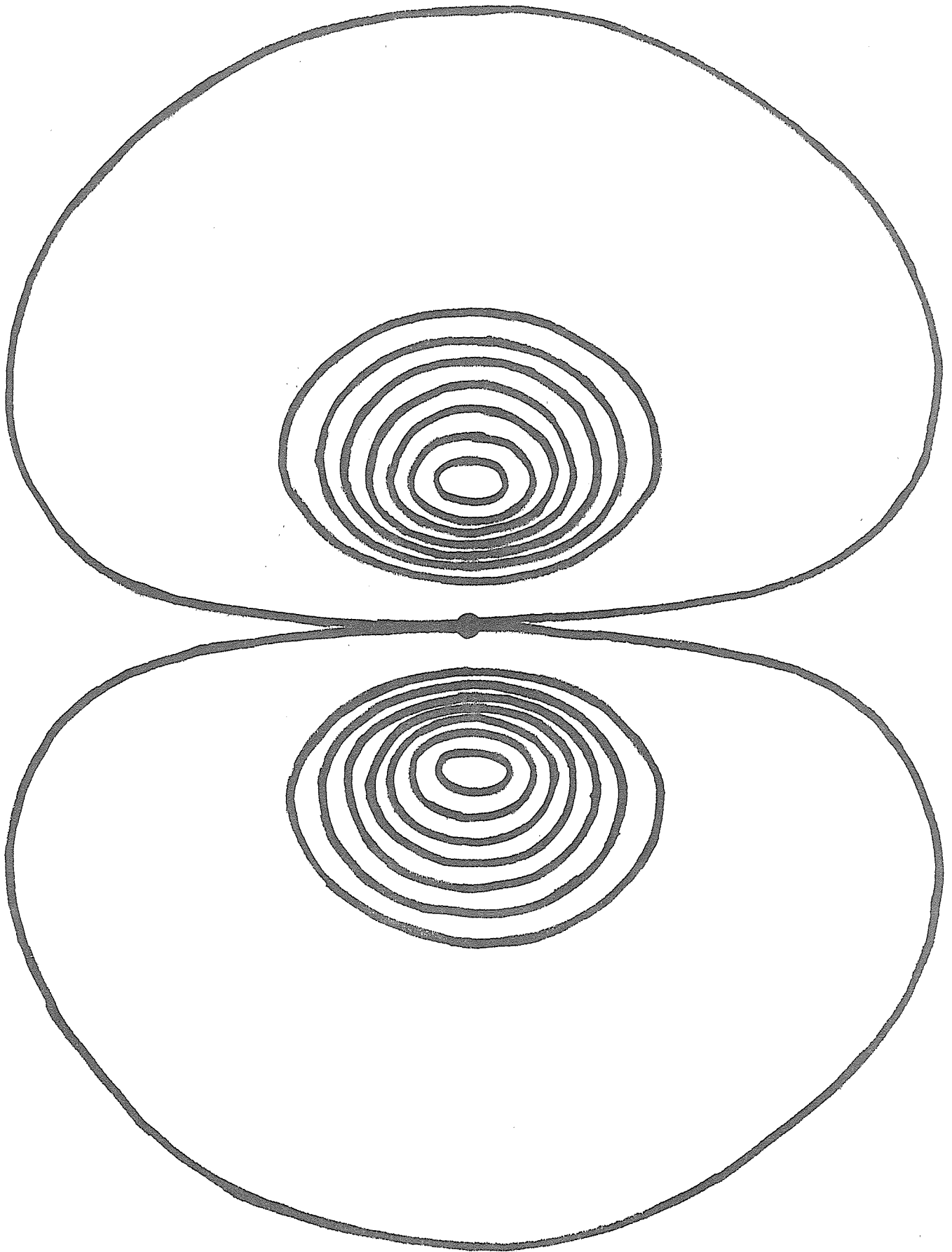


Figure 8. Contributions to the contragradience energy for the frozen π -bond in ethylene^{5c} ($\text{H}_2\text{C}=\text{CH}_2$). (The contour spacing is linear.)

- A. In the plane perpendicular to the plane of the molecule and passing through both C atoms.
- B. In the plane perpendicular to the plane of the molecule and bisecting the C-C distance.





D. Extrapolation to Larger Systems

In the preceeding sections, we have developed the basis for an understanding of the existence of chemical forces. This understanding has been based on calculations on very small systems using the GI³ and extended GI methods. The object of our analysis was to develop concepts which could be applied with confidence to systems too large for detailed calculations. The results of our analysis have two features which make them quite useful for such an extrapolation. First, the important quantity, the contragradience energy, is insensitive to self-consistency; it can be calculated to a high accuracy using only knowledge of the atomic states. Secondly, the contragradience energy can be expressed as a sum of pair energies, (see Eqns. 5), thus we need only calculate those terms which will change in any given process, dismissing the others as constant. We will illustrate the usefulness of the contragradience energy here by estimating the heights of the rotational barriers in ethane ($\text{H}_3\text{C}-\text{CH}_3$) and 2-butyne ($\text{CH}_3\text{C}-\text{C}\equiv\text{C}-\text{CH}_3$).

It is useful to discuss the interactions as pair interactions, and the concept of contragradience lends itself readily to this. The contragradience energy is simply the sum of pair terms of the form

$$C_{ij} = -D_j^i \langle \langle \nabla \phi_i | | \nabla \phi_j | - \nabla \phi_i \cdot \nabla \phi_j \rangle \rangle \quad (8a)$$

Here the D_j^i are just the one electron density matrices arising in the GI equations.³ Neglecting terms of second order in the overlap between orbitals involved in different bonds, the D_j^i for i and j in different bonds with i' and j' respectively can be shown to be

$$D_j^i = \frac{U_{(ij)} S_{ij}}{(1 + S_{ii'}^2)(1 + S_{jj'}^2)} \quad .$$

Thus, to a good approximation, we may rewrite Eqn. (8a) as

$$C_{ij} = - \frac{U_{(ij)} S_{ij}}{N} \langle \nabla \phi_i \parallel \nabla \phi_j \mid - \nabla \phi_i \cdot \nabla \phi_j \rangle \quad (8b)$$

where $U_{(ij)}$ is a constant arising from the spin-coupling of electrons i and j , and N is simply a normalization constant. For interactions involving orbitals in different bonds, $U_{(ij)} = \frac{1}{2}$. Assuming the overlaps within a bond to be 0.80, N is 2.70.

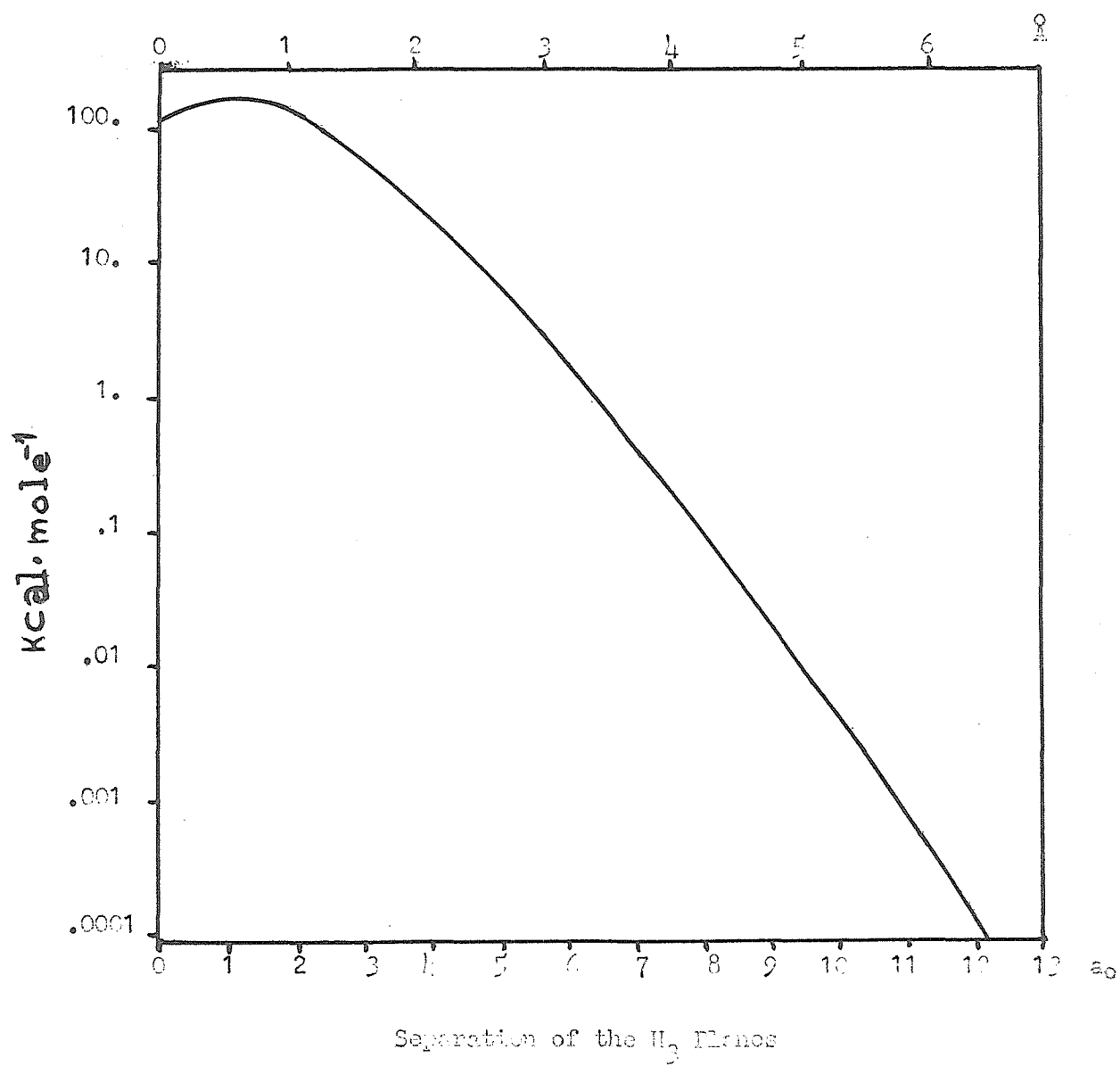
Having established the form of the interaction in the convenient form of the pair terms, let us begin by applying these concepts to the ethane molecule but using only atomic wavefunctions. Considering the frozen C atoms to be sp^3 hybridized, we can readily see that contributions to the rotational barrier may arise from the interaction of either of the C-H bonding orbitals of one methyl group with either of those in the other methyl group. Because of the cylindrical symmetry of the three sp^3 orbitals not involved in the C-C bond, we expect the interactions between the C sp^3 orbitals of the CH bonds of one methyl with those on the other methyl to make only a small net contribution to the rotational barrier. A somewhat larger effect should arise from the interactions of the H orbital part of the CH bonds of one methyl with

the $C\ sp^3$ part of the C-H bonds of the other. As will be discussed in detail below, this interaction will make also a negligible contribution to the rotational barrier in ethane. This leaves the interactions of the H orbitals of one methyl group with those of the other as the primary source of the rotational barrier. In Fig. 7 we show the change in the contragradience energy between eclipsed and staggered triangles of three H atoms as a function of the separation of the planes. The orbitals are frozen H atom orbitals, and the geometry of the three protons is assumed to be the experimental value for the methyl groups in ethane⁶ throughout. From Fig. 7, we see that the contragradience energy of the staggered form is $6.1\ \text{kcal}\cdot\text{mole}^{-1}$ lower than that of the eclipsed form (ethane corresponds to an H plane-H plane separation of $5.32a_0$ in Fig.7)⁶. Bearing in mind that the contragradience energy is only the dominant term in the binding energy, and generally is opposed by the other terms, we find our agreement with the experimental⁷ barrier height of $3.0\ \text{kcal}\cdot\text{mole}^{-1}$ to be excellent.

Now, let us consider the 2-butyne molecule; from Fig. 7, the H_3-H_3 interaction produces a barrier of $2.9\ \text{cal}\cdot\text{mole}^{-1}$ favoring the staggered conformer. But this is not all of the barrier!

Between the methyl groups there is a pair of triply bonded C atoms; a coupling of the motions of the methyl groups through this triple bond must be considered. Let us immediately dismiss the naive concept that the C-C triple bond is composed of a σ bond and two orthogonal π bonds. This bond should be regarded

Figure 7. Contribution of the H-H contragradience energy (in kcal·mole⁻¹) to the rotational barrier in ethane-like molecules as a function of the separation of the planes containing the three H atoms of the two methyl groups. An approximately normalized frozen wavefunction is used throughout. The geometry of the methyl groups is assumed to be the experimental equilibrium geometry in ethane.⁶



as three banana bonds. These arise from the three $C\ sp^3$ orbitals on each C which point at the other C. Each of these three orbitals on one C, call it A, will be coupled into a singlet with one of the orbitals on the other C, call it B. This is a highly attractive coupling; the coupling of each orbital of A with the other two sp^3 orbitals on B is repulsive. Thus, the sp^3 orbitals of A will be quite rigidly fixed with respect to those of B. Now let us consider the interaction of methyl groups with the orbitals of this triple bond. Consider one methyl group fixed in space, and allow the triple bond to rotate, neglecting the presence of the second methyl group. Because they are cylindrically symmetric about the same axis, the interaction of the $C\ sp^3$ orbitals of the methyl group with those of the triple bond may be regarded as negligible. Each of the orbitals of the triple bond is repulsively coupled to each of the H atom orbitals. This produces a barrier to the rotation of the triple bond favoring a staggered configuration between the orbitals of the triple bond and the H atoms of the methyl group. If we now freeze the configuration of this fragment, and allow the second methyl group to rotate, its motion is influenced by forces from the other methyl group both directly as in ethane, and through the triple bond. The first methyl group exerts a force favoring the staggered configuration, and a second force through the triple bond coupling toward the eclipsed configuration. The second force causes the free methyl group to align itself in a staggered configuration with the triple bond which is, in turn,

staggered with respect to the fixed methyl group. If the second force dominates, 2-butyne will be eclipsed, and if the first force dominates, it will be staggered.

Indeed, the molecule will be eclipsed; the barrier to this rotation is calculated⁸ to be $52.7 \text{ cal}\cdot\text{mole}^{-1}$. When the methyl groups are staggered, the triple bond will not actually be positioned as above; it will lie half-way between the methyl groups. This will lower the barrier somewhat. The contragradience energy contribution to the potential for rotation of a methyl group with respect to a C sp^3 orbital was found to be given by

$$C(\theta) = [1038 + 153\cos\theta + 58.9\cos 2\theta + 8.93\cos 3\theta] \quad (9)$$

in $\text{cal}\cdot\text{mole}^{-1}$. Application of Eqn. (9) shows that the barrier to rotation in this case is some $51.1 \text{ cal}\cdot\text{mole}^{-1}$. Thus, the net contragradience contribution to the rotational barrier in 2-butyne is $48.2 \text{ cal}\cdot\text{mole}^{-1}$ favoring the eclipsed configuration. This is in line with the experimental barrier height, $30 \text{ cal}\cdot\text{mole}^{-1}$, though the favored configuration has not been ascertained.⁹

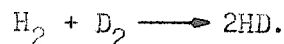
Finally, note that the contribution to the rotational barrier in ethane arising from the coupling of the H atoms of one methyl group with the sp^3 orbitals of the opposite methyl group is simply our original value for the coupling rotational barrier. The additional $52.7 \text{ cal}\cdot\text{mole}^{-1}$ is at least as small as the errors in the approximations, so these terms are, indeed, negligible.

Thus we see that we may make use of the dominance of the contragradience energy in chemical forces and the relative freedom

of the contragradience energy from the requirements of self-consistency to make reliable qualitative and semi-quantative predictions about systems far too large for GI calculations. This has been illustrated by approximation of the rotational barrier in ethane and a discussion of a mechanism for coupling of the rotational motion of the methyl groups through the C-C triple bond in 2-butyne.

THE REACTION SURFACE FOR
THE $\text{H}_2 + \text{D}_2 \longrightarrow 2\text{HD}$ FOUR-CENTER
EXCHANGE REACTION

Bauer and Ossa¹⁰ have interpreted their experimental data from shock tubes as indicating a four-center mechanism for the reaction



They find a vibrational preexcitation of $19 \text{ kcal}\cdot\text{mole}^{-1}$ to be required, and an activation energy of $42 \text{ kcal}\cdot\text{mole}^{-1}$. Both the experiment and their interpretation of it might justifiably be criticized,¹¹ but if the reaction does occur, a theoretical study of it as the prototype of a large class of chemical reactions would be of great interest. Rigorous quantum mechanical calculations of this reaction surface have been carried out.¹²⁻¹⁶ All of these show a barrier height of approximately $120 \text{ kcal}\cdot\text{mole}^{-1}$ in distinct disagreement with Bauer and Ossa's interpretation of their experiment.

Semi-empirical calculations¹⁷ of the surface indicate a barrier height of $62 \text{ kcal}\cdot\text{mole}^{-1}$ essentially in agreement with the interpretation of the experiment. An improved semi-empirical technique¹⁸ based on the contragradience energy shows a barrier height of $113 \text{ kcal}\cdot\text{mole}^{-1}$.

A. The Shape of the Surface

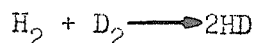
Wilson and Goddard¹³ have carried out minimum basis set configuration interaction calculations on the potential energy hypersurface on which this reaction would occur for a number of possible transition state geometries. This study included the first several electronic states of the square, tetrahedral, centered-equilateral triangular, rhombic, kite-shaped, linear, and trapezoidal configurations; it showed that the lowest possible transition state was in the vicinity of the square configuration. Several reaction channels are open to the system in this transition state region. Because the energy throughout this region is significantly above that of an H_2 molecule and two H atoms (within the same approximation), several of these channels lead to that limit rather than to two H_2 molecules. The channel through which the reaction will proceed depends on the vibrational phase of the reactants. In the region of the square, for example, if the system vibrates back into a rectangle or into a trapezoid it enters the four-center exchange channel. On the other hand, if it vibrates into a rhombic or a kite-shaped configuration first, the system enters a dissociative channel. In the neighborhood of the transition state, these channels are coupled, the rectangular and trapezoidal configurations are the same channel. At short distances the restoring force for the mode of vibration from the four-center exchange channel into the dissoci-

ative kite-shaped channel remains negative, the restoring force for the vibration of the rhombic configuration into the kite-shaped configuration is also negative. Thus the vibrational phase of the several modes of the system are all important in determining the channel through which the reaction will proceed, and thereby the products of the collision.

While the absolute error in the total energy determined by minimum basis set calculations is large, the relative error between two points on an energy surface is usually more reliable, and such calculations have been shown to lead to reliable equilibrium geometries for bound molecules.¹⁹ Recently calculations^{12,14-16} with larger basis sets on some of the same regions of the surface by a number of techniques have become available for comparison to our minimum basis set results. Conroy and Malli¹² have considered the rectangle and square portions of the surface and obtained a far lower total energy, but essentially the same barrier height. Rubenstein and Shavitt¹⁴ have considered several geometries and concluded that the transition state would be in the vicinity of the square if their barrier height weren't as high as it is, which is also in agreement with the minimum basis set result. The large basis set calculations of Silver, Stevens, and Kurlus¹⁵ are reported¹⁴ to also be in substantial agreement with these results. Finally, large Gaussian basis set spin-coupling optimized GI²⁰ calculations¹⁶ on the rectangular configurations indicate the same barrier height. The extraordinary agreement between these results--each with a differ-

ent quantum mechanical approximation technique--reinforces our confidence that the shape of the calculated surface is reasonably close to that of the actual surface and that the calculated barrier height is appropriate for the actual four-center mechanism.

Under the increasing weight of theoretical evidence¹²⁻¹⁶ that the barrier to the four-center exchange reaction



is on the order of $120 \text{ kcal} \cdot \text{mole}^{-1}$, we are forced to suggest that whatever (if anything) Bauer and Ossa¹⁶ are observing in their shock tubes with an activation energy of $42 \text{ kcal} \cdot \text{mole}^{-1}$, it is not this four-center mechanism. Furthermore, the semi-empirical calculations¹⁷ which find the activation energy to be $62 \text{ kcal} \cdot \text{mole}^{-1}$ must also be wrong. (See Proposition III for a discussion of an improved semi-empirical scheme based on the contragradience energy, which gives a barrier height of $113 \text{ kcal} \cdot \text{mole}^{-1}$.)

B. Contragradience and the Energy Surface

We have seen above that chemical forces may conveniently be considered as arising from changes in the contragradience energy. The chemical forces and the shape of the reaction surface are directly related. In order to understand the shape of the surface, we will examine the contragradience energy surface for this reaction (see Appendix A). Comparing the results for the fully self-consistent wavefunction with those for a frozen wavefunction, we will find that the detailed shape of the reaction surface in the region of strong interaction is highly dependent on self-consistency. The differences are attributable predominantly to the incorporation of nodes in the self-consistent orbitals which severely lower S_{ij} in Eqn. (8b).

The shape of the frozen surface for a rectangular configuration, is significantly different from that of the self-consistent surface: the minimum energy path on the frozen surface corresponds to stretching of the optimum bond length from its separated molecule limit ($1.6a_0$) as the second molecule approaches. This path passes through the square configuration between $2.0a_0$ and $2.2a_0$. On the other hand, the minimum energy path on the self-consistent surface corresponds to a shrinkage^{12,16} of the optimum bond length from its separated molecule limit, as the second molecule approaches. This difference in shape arises from the inability of the frozen

wavefunction to emulate the effect of the nodes in the self-consistent wavefunction, especially in the diagonal interaction which is not affected by changes in the spin-coupling.¹⁰

A detailed examination of the contragradience energy shows that this shrinkage may be quite common in nonreactive collisions. We will illustrate this here by considering the collision of an H atom and an H₂ molecule both in the reactive linear configuration and in the non-reactive approach of the atom along the perpendicular bisector of the molecule.

At large separations of the H and the H₂, the optimum size of the H₂ molecule will be determined, primarily, by the contragradience of its orbitals. From Eqn. (8a), we see that the contragradience energy of this pair is given by

$$C_{12} = -D_2^1 \langle \nabla \phi_1 \| \nabla \phi_2 | - \nabla \phi_1 \cdot \nabla \phi_2 \rangle.$$

In Fig. 8, we see that the contragradience of the H₂ orbitals,

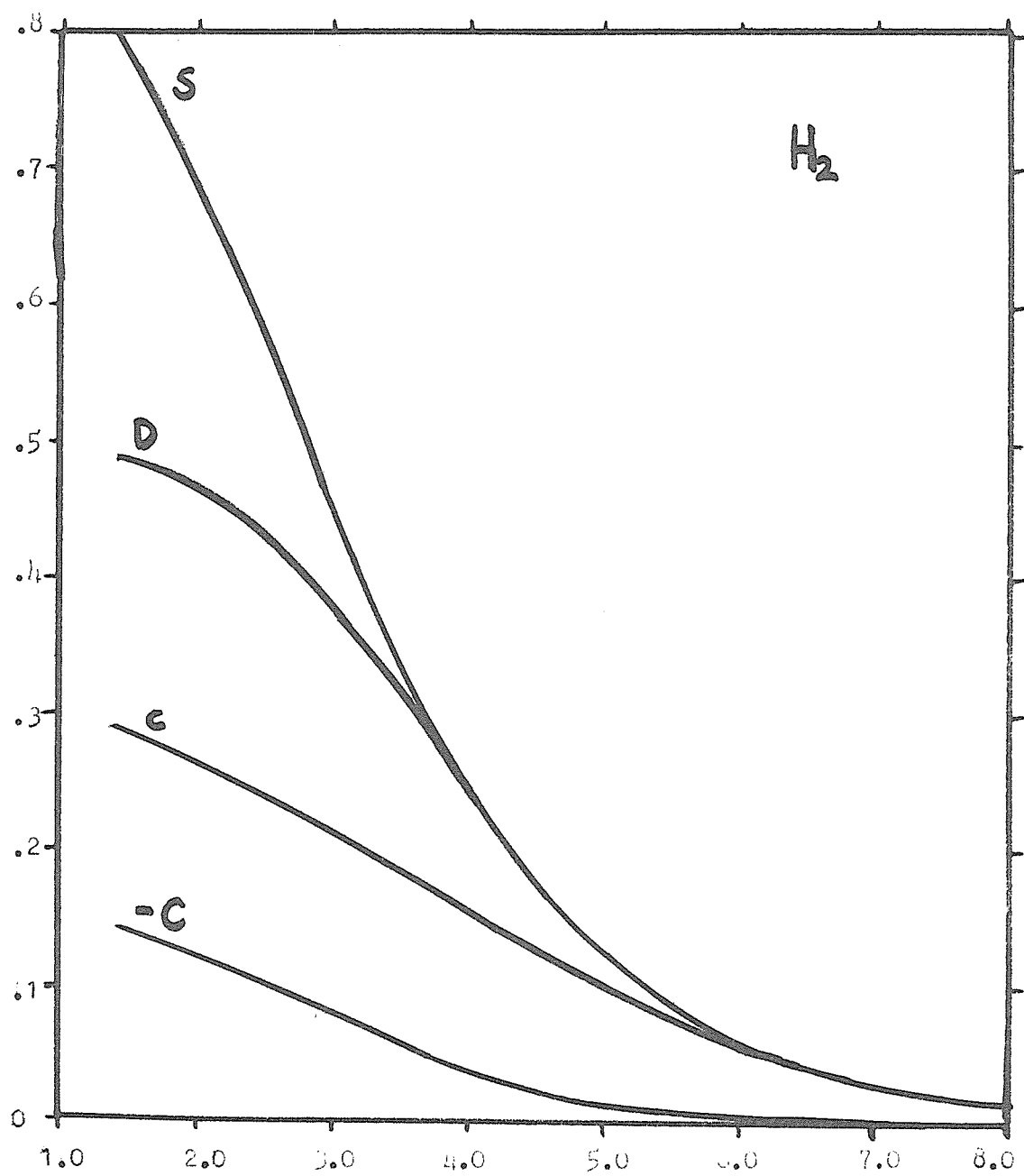
$$\langle \nabla \phi_1 \| \nabla \phi_2 | - \nabla \phi_1 \cdot \nabla \phi_2 \rangle$$

is relatively insensitive to changes in the internuclear separation (especially near R_e), and therefore may be regarded as a constant here. Thus the variations in C₁₂ will follow those in D₂¹. The variations in D₂¹ depend on the squares of the various intermolecular overlaps, thus at a bond length of r, and an intermolecular separation of R, D₂¹ is given by

$$D_2^1(R,r) = D_2^1(\infty,r) \left[1 + \sum_{k=1}^2 \sum_{l,j=1}^2 K_{k,l,i,j} S_{li}(R,r) S_{kj}(R,r) + O(S^3) \right] \quad (10)$$

where the {K} are positive constants. From Eqn. (10), we see that the minimum in the contragradience energy at a given R will be shif-

Figure 8. The contragradiance, the contragradiance energy, the overlap, and the density matrix for the ground $^1\Sigma_g^+$ state of H_2 as a function of the internuclear separation. (Minimum basis set results are used throughout.)



ted from its position at infinite separation in the direction which raises the intermolecular overlap terms. Because of the dominance of C in the binding energy, we would expect the optimum bond length to change in the same direction.

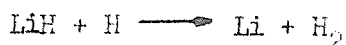
In the perpendicular approach of an H atom to the H_2 molecule, these overlap terms are maximized by a shortening of the bond length and we would expect the molecule to shrink. (A shrinkage of $0.004a_0$ in the H_2 bond length has indeed been observed at an intermolecular separation of $3.6a_0$.) In the linear approach, the overlap of the H atom orbital with the H_2 orbital localized about the closest H dominates in Eqn. (10). In order to increase this overlap, the molecule must stretch toward the H atom.

Applying the same reasoning to the collision of two H_2 molecules immediately suggests that they will shrink in a rectangular approach and expand in a linear one.

At smaller separations, the intermolecular $\{C_{ij}\}$ become as important as C_{12} in determining the behavior of the system. These $\{C_{ij}\}$ depend on the intermolecular overlaps in a linear rather than a quadratic fashion. They are repulsive in the cases we are considering here, hence their minimization is paramount to the stabilization of the system. The system will generally change its spin-coupling to minimize these interactions, the ability or inability of the system to do this determines the height of the energy barrier, and, hence, whether the collision will be reactive or non-reactive.

Let us now consider these changes in detail. At infinite separation, the orbitals of the H_2 molecule are coupled into a singlet, and the H atom orbital is coupled to this singlet to produce a doublet. In the linear collision, the transition state is symmetric, the electronic state has $^2\Sigma^+$ symmetry. Pulling the transition state apart symmetrically, we find it must dissociate to three H atoms, each in its ground state. Clearly the product of three H atom orbitals does not transform into minus itself under any symmetry operation, hence the coupling of the orbitals must produce the proper symmetry. The spatial part of the electronic wavefunction must transform into minus itself under the interchange of the outer orbitals, hence these must be anti-symmetrically coupled. Thus the spin-coupling of the transition state at infinite separation (and, indeed, at any separation for localized orbitals) must be that of two orbitals coupled into a triplet, and the third coupled to this triplet to yield a doublet. The spin-coupling must change from a singlet coupled with a doublet to a triplet coupled with a doublet during the course of the reactive linear collision.

While this behavior might, at first, appear to be atypical, and simply the result of the unusually high symmetry of the transition state, we doubt it. The equivalent binding of the central atom to the two outer atoms is central to the intuitive concept of a transition state. Furthermore, this type of behavior has also been observed²¹ along the reactive linear approach in the reaction

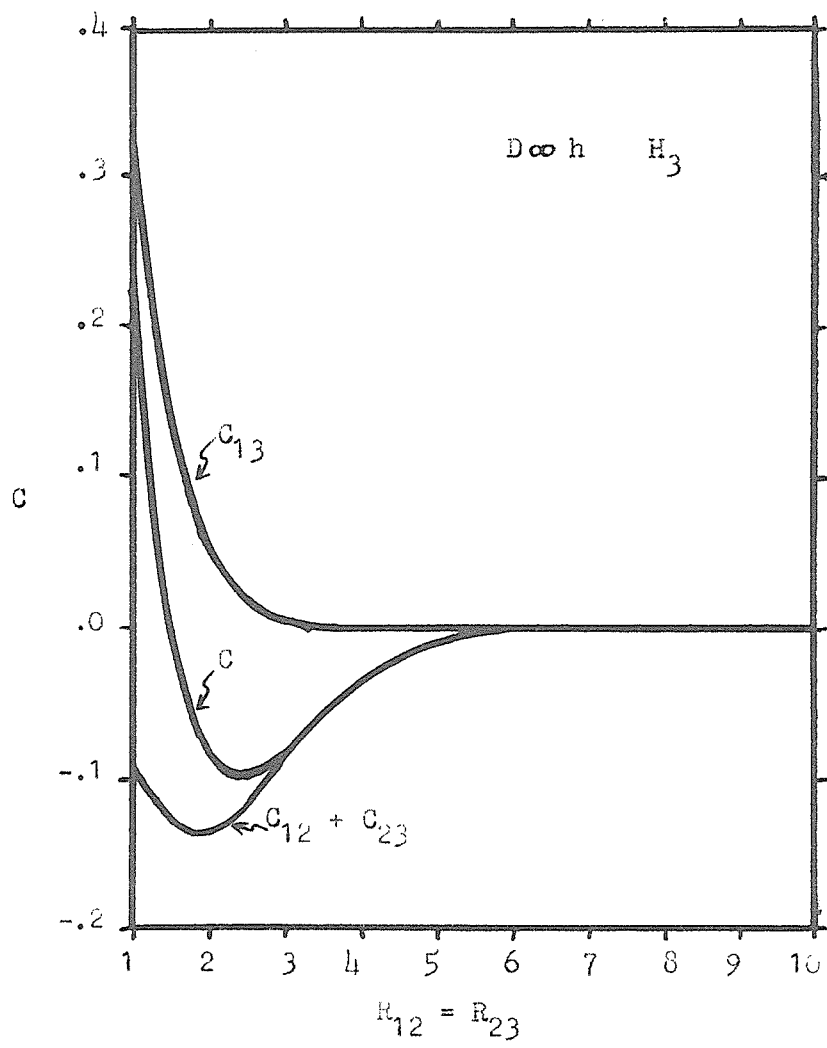


where it is not induced by symmetry.

The continuous change of the spin-coupling during the linear approach of the H atom to the H₂ molecule augments the stretching which we saw at large separations above. Consider the transition state during the approach: $U_{(12)}$ (see Eqn. 8b) changes from +1 to $+\frac{1}{2}$ while $U_{(23)}$ changes from $-\frac{1}{2}$ to $+\frac{1}{2}$. The attractive part of the contragradience energy, $C_{12} + C_{23}$, exhibits a minimum at essentially the same separation as that in C_{12} at infinite intermolecular separation (see Fig. 9). The repulsive term, C_{13} , depends on the separation of the outer atoms (rather than on that of neighboring atoms as for the attractive terms) thus the maximum in C_{13} occurs at smaller internuclear separation than the minimum in $C_{12} + C_{23}$. Since C_{13} is decreasing with R in this region it tends to move the minimum in the total contragradience energy to a larger separation, (see Fig. 9), hence we expect the molecule to stretch in the reactive collision.

The nonreactive collision is somewhat different. In a non-reactive collision there exist significant repulsive terms which cannot simultaneously be satisfactorily dealt with by a change in the spin-coupling, even though the spin-coupling may change in the same manner as for a reactive collision (it does exactly this in the rectangular configuration of H₄).²² In these cases, the above trends continue until the intruding molecule comes so close that the repulsive intermolecular terms swamp out C_{12} , and the atoms of the molecule are forced away from the intruder. This short-range

Figure 9. Contragradiance energy and composite pair' terms for $^2\Sigma^+$
 H_3 as a function of interatomic separation. (A frozen
wavefunction is used throughout.)



effect is diametrically opposed to the long-range effect described above; thus, we should expect the optimum bond length as a function of intermolecular separation to exhibit a minimum for the isosceles triangular configuration of H_3 as well as for the rectangular configuration of H_4 . On the other hand, a maximum should occur for linear H_4 .

The minimum in the optimum bond length for rectangular H_4 as observed on the frozen surface and the SCF surface suggests that the shape of the frozen surface is not in error, these effects simply occur at too large a separation there because of the crudeness of the wavefunction.

Thus consideration of the contragradience energy allows us to readily understand the detailed shape of the relatively complicated energy hypersurfaces on which reactions occur.

S U M M A R Y

In an examination of the binding energies of a number of small chemical systems, both bound and unbound, we have isolated one term which dominates the binding energy in every case. This term, the contragradience energy, is relatively insensitive to self-consistency, thus we should be able to make use of it with confidence in systems far too large for self-consistent calculations (a few examples were treated). The sign of its changes is predictable from consideration of the spin symmetry of the system and its constituent parts without detailed numerical calculations. Since it allows a discussion of binding energy in terms of pair effects, it is possible to break up the intermolecular and interbond interactions into units which may be conveniently discussed.

Conceptually the dominance of the contragradience energy is quite gratifying as it derives its magnitude from the opposition of the gradients of orbitals localized on different centers. That is, the perturbation on atomic stability responsible for the stability or instability of molecules arises from their multi-centered nature.

Using the contragradience energy, we have been able to understand chemical binding, resonance, rotational barriers, and the shape of reaction surfaces. In addition, the contragradience leads

directly to a natural definition of a bond region whose shape, location, and general behavior is in agreement with empirically based concepts.

REFERENCES

1. C.W. Wilson, Jr. and W.A. Goddard III, a) Chem. Phys. Lett., 5, 45, (1970); b) "The Role of Nonclassical Kinetic Energy and Contragradience in the Chemical Bond", J. Chem. Phys., to be published; c) Bull. Am. Phys. Soc., 14, 1192 (1969).
2. Atomic units are used throughout this thesis. In these units, the charge and mass of the electron are -1 and 1 respectively, the unit of energy is the hartree (1 hartree = 627.51 kcal mole⁻¹ = 27.211eV) and the unit of length is the bohr (1 bohr = 0.52917⁰Å). (E.R. Cohen, and J.W. DuMond, Rev. Mod. Phys., 37, 537 (1965).)
3. W.A. Goddard III, Phys. Rev. 157, 81 (1967).
4. Note that for the self-consistent case for H₂⁺, ϕ_{1s}^L and ϕ_{1s}^R (Eqns. 6a and 6b) cannot be determined from a variational expression. The curve labeled \bar{T}^x in Fig. 2 arbitrarily selects ϕ_{1s}^L to be the 1s orbital on the left center, and ϕ_{1s}^R that on the right. Several other definitions of ϕ_{1s}^L and ϕ_{1s}^R lead to substantially the same results. The same nonuniqueness problem has been noted by Feinberg, Ruedenberg and Mehler (to be published; we thank Dr. Ruedenberg for a copy of this paper prior to publication). This problem does not arise for the cases involving more electrons.
5. a) The author wishes to thank Mr. Richard J. Blint for the use of his Li₂ wavefunction. b) The author wishes to thank Dr.

William E. Palke for the use of his LiH wavefunction. c) The orbital exponent, 1.5679, is taken from an optimized minimum basis calculation on the C atom. (E. Clementi and D.L. Raimondi, J. Chem. Phys. 38,2686 (1963)).

6. All geometric parameters are taken from R.T. Morrison and R.N. Boyd, Organic Chemistry, Allyn and Bacon, Inc., (Boston),1959.

Additivity of bond lengths is assumed.

7. J.D. Kemp and K.S. Pitzer, J. Chem. Phys. 4,749 (1936); K.S. Pitzer, Discussions Faraday Soc. 10,66 (1951); D.R. Lide, J. Chem. Phys. 29,1426 (1958).

8. The geometric parameters are from Ref. 6. The orbital exponents are those for an optimized minimum basis set calculation on the C atom.⁵ All analytic integrals are taken from M. Kotani, A. Amemiya, E. Ishiguro, and T. Kimura, "Table of Molecular Integrals", Maruzen Co. Ltd., (Tokyo,1963).

9. R. Kopelman, private communication, and P.R. Bunker and H.C. Longuet-Higgins, Proc. Roy. Soc. (London),A280,340 (1964); and R. Kopelman and R.S. Halford, unpublished work.

10. S.H. Bauer and E. Ossa, J. Chem. Phys. 45,434 (1966).

11. The use of a platinum coated thermocouple in these experiments may lead to significant, concentration dependent, systematic errors in the measurement of the temperature in the shock tube as well as in the measured concentration of reactants. The fit of their data to their mechanism is poor, and hardly acceptable for eight parameters. The most convincing evidence against the free radical

process occurring is the linear dependence of the reaction rate on the concentration of the carrier gas Ar; this might simply indicate catalysis by an impurity present in the Ar, e.g. O_2 .

12. H. Conroy and E. Malli, J. Chem. Phys. 50,5049 (1969).
13. C.W. Wilson, Jr. and W.A. Goddard III, J. Chem. Phys. 51,716 (1969).
14. M. Rubenstein and I. Shavitt, J. Chem. Phys. 51,2014 (1969).
15. D. Silver, R. Stevens, and M. Karplus, to be published.
16. See Appendix A, this is to be published as C.W. Wilson, Jr. and W.A. Goddard III, "Ab Initio Quantum Mechanical Calculations on the $H_2 + D_2 \longrightarrow 2HD$ Four-Center Exchange Reaction Surface II. Orbitals, Contragradience and the Surface."
17. a) H. Eyring, J.A.C.S. 53,2537 (1931); b) S.W. Benson and G.R. Haugen, J.A.C.S. 87,4036 (1965); c) K. Morokuma, L. Pedersen, and M. Karplus, J.A.C.S. 89,5064 (1967); and d) R.B. Abrams, J.C. Patel, and F.O. Ellison, J. Chem. Phys. 49,450 (1968).
18. C.W. Wilson, Jr., to be published. (See proposition III.)
19. For example, the rotational barrier in ethane is predicted well by a minimum basis set calculation. [See O.J. Sovers, C.W. Kern, R.M. Pitzer, and M. Karplus, J. Chem. Phys. 49,2592 (1968) and references therein.]
20. R.C. Ladner and W.A. Goddard III, J. Chem. Phys. 51,1073 (1969).
21. R.C. Ladner, private communication.
22. C.W. Wilson Jr., unpublished work.

A P P E N D I X A

Ab Initio Calculations on the $H_2 + D_2 \rightarrow 2HD$ Four-Center
Exchange Reaction. II. Orbitals, Contragradience Energy,
and the Reaction Surface*

C. WOODROW WILSON, JR.,[†] and WILLIAM A. GODDARD III[‡]

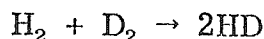
Arthur Amos Noyes Laboratory of Chemical Physics**

California Institute of Technology

Pasadena, California 91109

(Received)

We discuss the reaction surface for the four-center exchange reaction



using techniques which furnish independent particle orbitals (the spin-coupling optimized GI orbitals). The surface is comparable to previously published surfaces determined by configuration interaction. The shape of the surface is explained by the same arguments which have previously been used to explain the bonding or nonbonding of molecules.

*Partially supported by grants (GP-6965 and GP-15423) from the National Science Foundation.

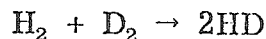
[†]National Science Foundation Trainee.

[‡]Alfred P. Sloan Fellow.

**Contribution No. 4029.

I. INTRODUCTION

Previous ab initio quantum mechanical determinations¹⁻³ of the



four-center exchange reaction surface have consistently shown a barrier height of approximately 125 kcal/mole although several basis sets and quantum mechanical approximations were used. Where they overlapped, these surfaces agreed that the transition state was a distorted square, most likely a trapezoid. All agreed that the energy of the transition state was above that of one molecule and two atoms, making the reaction through this mechanism quite unlikely. These calculations indicated a reaction surface of the type shown in Fig. 1a.

In order to understand the shape of this energy surface, we will first consider the surface determined by a simpler wavefunction. In Fig. 1b we show the energy surface which results when we freeze the orbitals to be H atom 1s orbitals on each center and optimize the spin-coupling between them. (We shall refer to this wavefunction as the frozen wavefunction throughout this paper.) Then we will consider the spin-coupling optimized GI wavefunctions and examine the changes in the surface due to self-consistency.

Conroy and Malli¹ noted that the minimum energy bond length of the constituent H_2 molecules appeared to decrease when the molecules were brought together; the same behavior is observed in Fig. 1a. We will examine this behavior to show that it arises naturally from the forces which cause the chemical bond, and we will find that it could occur in many other nonreactive collisions as well.

II. CALCULATIONAL DETAILS AND ORBITALS

The wavefunction is written as

$$G_1^{\gamma L}[\phi_1 \phi_2 \phi_3 \phi_4 \alpha\beta\alpha\beta], \quad (1)$$

where the group operator $G_1^{\gamma L}$ ensures that the total wavefunction has the correct spin symmetry (singlet) and satisfies Pauli's principle. The orbitals in (1) are all functionally optimized and the spin-coupling in the group operator is optimized simultaneous with the orbitals. The resulting method is called the Spin-Coupling Optimized GI (or SOGI) method and the orbitals are referred to as the SOGI orbitals (or else just the GI orbitals). At large IMD (and smaller BL) ϕ_1 and ϕ_2 are localized on one H_2 (say the left one) and ϕ_3 and ϕ_4 are equivalent and localized on the other H_2 . The orbitals ϕ_1 and ϕ_2 are then essentially just like the orbitals of H_2 with one more localized near one proton and the other orbital more localized near the other proton. A contour plot of one of these orbitals is given in Fig. 2a where we see that the second H_2 has slightly perturbed the orbital by introducing a nodal plane in the tail of the orbital. Thus the four GI orbitals are

equivalent but localized near different protons. As the IMD is decreased the orbitals change as shown in Fig. 2b until at the square configuration the orbitals have the form given in Fig. 2c. In this case at square configuration the optimum coupling of the orbitals is the GF-like coupling in which ϕ_1 and ϕ_3 (localized on diagonally opposite protons) are coupled into a triplet and ϕ_2 and ϕ_4 are coupled into a triplet and then the four orbitals coupled together into the correct singlet wavefunction. In the case of exact GF-like coupling the wavefunction is antisymmetric in ϕ_1 and ϕ_3 and one would expect the choice of ϕ_1 and ϕ_3 to not be unique. However for spin-couplings which are exactly GF the orbitals are determined uniquely and thus the unique form of the GF orbitals can be obtained by solving for the orbitals as a function of the spin-coupling and taking the limit.

Actually as shown in Ref. 6, if the orbitals are allowed to be inequivalent then for configurations very near the square the spin-coupling angle deviates from the GF value and the orbitals change so that the new ones $\{\phi'_i\}$ are nearly exactly symmetric and antisymmetric combinations of the old antisymmetrically coupled pairs. However the resulting energy drop is only .000061h for a square of side $2.6 a_0$ and this change occurs only right near the square configuration and so we will ignore this effect in discussing the orbitals.

The SOGI equations were solved using expansions in terms of nuclear centered Gaussian functions chosen to give a good description of the H_2 molecule over a wide range of internuclear separations. (At $R_e = 1.425 a_0$, it gives an energy of $-1.148454 h$ and for the H atom, an. energy of $-.499921 h$.)⁵ The quadratically convergent SOGI program was used in which the SOGI equations are solved including first-order corrections in the SOGI one-particle Hamiltonian.

III. CONTRAGRADIENCE AND CHEMICAL BINDING

Before proceeding with our analysis, we will digress to outline the factors which determine whether or not a chemical system will be bound.⁷ (These concepts are discussed more fully elsewhere.^{7c}) In the examination of a number of chemical systems, both bound and unbound, it has been found that the binding energy closely parallels the nonclassical or exchange part of the kinetic energy, which we will denote by T^X ,

$$T^X = T - T^{Cl}, \quad (1a)$$

where T is the total kinetic energy of the system and

$$T^{C\ell} = \sum_i \langle \phi_i | t | \phi_i \rangle \quad (1b)$$

is the kinetic energy of the Hartree-like exchangeless wavefunction using the GI orbitals. Using Eq. (1b) in (1a) leads to^{7c}

$$T^X = \sum_{i>j} D_j^i S_{ij} [\langle \phi_i | t | \phi_i \rangle + \langle \phi_j | t | \phi_j \rangle - \frac{2}{S_{ij}} \langle \phi_i | t | \phi_j \rangle], \quad (1c)$$

where the D_j^i are just the one-electron density matrices appropriate for singly occupied nonorthogonal orbitals (the spin-coupling is explicitly contained in the D_j^i). Other one-electron properties can be written in the same form as Eq. (1c) by replacing the t operator by the appropriate operator. The reason for the dominance of T^X in the binding of molecules is the vector dot-product nature of the t operator. When ϕ_i and ϕ_j are on different centers, the third term (called the interchange term) enhances rather than cancels the first two terms because of this vector dot product operator. This is because the gradients of the two orbitals are then opposed throughout the region of the major contribution to the interchange term. Thus the interchange term adds to the noninterchange terms with the same sign rather than the opposite sign. This contragradient nature of orbitals on different centers can be expressed by a quantity called the contragradience

$$c_{ij} \equiv \int d\tau [|\nabla \phi_i| |\nabla \phi_j| - \nabla \phi_i \cdot \nabla \phi_j] \quad (2a)$$

The contragradience contribution to the energy is

$$C \equiv - \sum_{i>j} D_{ij} c_{ij} \equiv \sum_{i>j} C_{ij} . \quad (2b)$$

This term dominates the binding energy in both bound and unbound situations. This energy will be referred to as the contragradience energy or just the contragradience. We found previously that the contragradience of the orbitals on different centers leads to large C_{ij} and that the pairing of the orbitals determines the sign of D_{ij} and hence whether the pair contribution C_{ij} will be binding or antibonding. For example, for H_2 with the singlet pairing, $D_{ij} > 0$ and the singlet is bound, but for the triplet $D_{ij} < 0$ and the triplet is not bound.

The dominance of C on the energy surface is illustrated in Fig. 3 where we compare the contragradience energy and energy as a function of bond length (BL) for fixed IMD.⁹ At small BLs, other terms in the energy lead to repulsive forces which counter C and eventually balance it leading to a minimum in E before that in C .

The density matrix can be written as

$$D_j^i = U_{(ij)} S_{ij}/N + O(S^2) \quad (3)$$

where N is just a normalization constant and $U_{(ij)}$ is determined by the spin coupling of the pair ij . We will find (3) to be useful in our analysis of the contributions to the contragradience energy.

IV. ANALYSIS OF THE SURFACE

From Fig. (1b) we see that the minimum energy path on the frozen orbital surface (FOS) goes smoothly toward the square as the intermolecular distance (IMD) is shortened toward approximately $2.1a_0$. From Fig. (4b), it is evident that the dominating factor in this expansion of the BL is a large positive change in C at smaller bond lengths (BL) and IMD's. From Figs. (4b), (5b), and (6b), we see that this is due to the dominance of the changes in the repulsive $\{C_{ij}\}$ s--those along the diagonals, and those along the long sides of the rectangle--over the attractive $\{C_{ij}\}$ s--those along the short sides. It is these large repulsive terms which self-consistency must minimize to lower the energy of the system.

Next we examine the contragradience energy for the self-consistent wavefunctions to discover how the differences in the surfaces arise. This reaction surface, shown in Fig. (1a), is constructed from fully self-consistent solutions of the spin-coupling optimized GI (SOGI) equations.

From Figs. (4), we see that the significant deviation between these surfaces is largely due to the highly different behavior of the contragradience energies of the SCF and frozen wavefunctions. For example, for an IMD of $2.2a_0$, the change in C for BL varying from 1.4 to $2.2a_0$ is $+0.10$ for the SCF surface (see Fig. 4a), and $.07$ hartrees for the FOS (see Fig. 3b). At a molecular separation of $3.2a_0$.

the molecules are forced away from the square by the contragradience on both surfaces, a change of .15 hartrees on the FOS and .20 hartrees on the SCF. At the same time, the repulsive interactions for a given nuclear configuration will be less sensitive to self-consistency. Since these repulsions are important in determining the optimum separation, the general pattern of lowering of C over the SCF surface, especially at smaller BLs, suggests that the optimum BL may shrink as the IMD is decreased. We will consider this point in greater detail below.

We will now examine the changes in the individual pair-contragradience energy terms to determine how self-consistency changes the shape of the surface. (We will see here that the changes in the contragradience energy are consistent with those in the binding energy, thus re-enforcing our previous conclusion⁷ that chemical binding could reasonably be considered as arising from the contragradience energy.)

We begin with the simplest case, that of the pair $(\phi_1$ and $\phi_3)$ correlated along the diagonal (see Figs. 5). For the frozen case, we have hydrogen atom orbitals on the two opposite corners, and therefore, a large region over which the contribution to c_{13} is significant. Both c_{13} and S_{13} are large over the region of interest, thus C_{13} makes a significant contribution to the energy; from Eq. 3, D_3^1 is positive, thus this contribution is repulsive. For this interaction, $U_{(13)} = -\frac{1}{2}$ throughout, thus the contours of constant C_{13} deviate from circles primarily because of the variations in the normalization constant in Eq. (3).

Examining the SCF orbital (Fig. 2), we see that very little change has been made in c_{13} , the integrand still arises essentially from

just two 1s-type functions at opposite ends of the diagonal. On the other hand, Fig. (5a) shows that C_{13} changes significantly, becoming far less repulsive for small BL's and IMD's. This decrease results almost entirely from the lowering of S_{13} in Eq. (3), the decreased overlap arises from the inclusion of a node in the tail of the orbital near the other molecule. The occurrence of this node near the other molecule allows a highly effective cancellation of overlap in the repulsive cases while maintaining a high overlap within the molecule. This cancellation is seldom below 50% of the frozen orbital value over the region of the surface illustrated, growing to over 80% for the smallest IMD's and BL's shown. Thus the highly repulsive interaction of the orbitals at the opposite ends of the diagonal is significantly lessened in the SCF case by the introduction of a node in the orbital near the other molecule and placed in a manner such that the effect is on the repulsive interactions.

Now we consider the case of the repulsive interaction arising in the FO case from the two hydrogen atom orbitals (ϕ_1 and ϕ_4) located at opposite ends of the long side of the rectangle (Figs. 6). Here again and for the same reasons both c_{14} and S_{14} are large, making the contribution of C_{14} significant. For small BL, the $U_{(14)} \approx -\frac{1}{2}$ making C_{14} repulsive, while near the square, the $U_{(14)} \approx +\frac{1}{2}$ making C_{14} attractive; this amounts to a change of some .20 hartrees along the $\text{IMD} = 2.2 a_0$ line from a BL of $1.2 a_0$ to square. The subtle changes in the wavefunction responsible for this problem are obvious from the orbital

shown in Fig. (7). The significant flattening of the SCF C_{ij} surface for smaller BL's arises from the presence of the node in the orbital. The cancellation of overlap is not quite so efficient here as in the case above, only reaching 78% for the smallest IMD's and BL's illustrated.

Near the square, a second phenomenon occurs for the C_{14} surface in both the FO and the SCF cases: Quite simply, this pair term, C_{14} , slides towards being the bonding interaction, exchanging roles with the original bonding interaction. This all happens as the $U_{(14)}$ changes from its repulsive $-\frac{1}{2}$ value to its attractive $+\frac{1}{2}$ value near the square. (This change was found to occur here within 0.1 bohr of the square.) As we see from Fig. (2), in the vicinity of the square, the orbitals begin to look much the same along the long and short sides of the rectangle. This allows only a quite small decrease in c_{14} in the same way as will be discussed for the attractive interaction along the short side below. The build-up of amplitude between the centers here effectively counteracts the presence of the node, and as a result only very small changes (less than 2%) occur in the overlap near the square.

Finally, let us consider the interaction, C_{12} , which is originally attractive, that along the short side of the rectangle (Figs. 6). On the frozen surface at small BL, $U_{(12)} \approx 1$ and C_{12} decreases with the IMD because of the terms of $O(S^2)$ in Eq. 3, since S_{12} is quite large here. Near the square, $U_{(12)}$ changes quite rapidly to a value of $+\frac{1}{2}$, overwhelming this drop and forcing a minimum in C_{12} away from the square. Then C_{12} changes continuously across the square line into the repulsive interaction discussed above.

It would be sufficient for the SCF surface to hold this shape. However, the higher order terms which result in the shape of the frozen surface are sharply decreased by the decreases in overlap required to lower the highly repulsive C_{ij} 's discussed above. This considerably flattens the C_{ij} surface in the region of small BL. The S_{12} is already large so only a small increase (5%) is allowed in it.

Since the SCF C_{12} surface in Fig. (6a) is still not quite what we might have expected at large IMD and small BL, we will examine its behavior more closely. We will see below that the terms which are quadratic in the intermolecular overlap are responsible for the observed shrinkage!

V. THE MINIMUM ENERGY PATH IN COLLISION PROCESSES

When two species approach one another, their interaction may be classified as either reactive or nonreactive. Except in the case in which both species are open-shell species, this distinction is only clear at small separations.

Let us consider the interaction of an H_2 molecule with an intruding species. At large separations the optimum BL of the molecule is determined by C_{12} . Near R_e , (for BL) c_{12} (see eq. 2b) is insensitive to variations in the internuclear distance, so the behavior of C_{12} is determined by that of D_2^1 . D_2^1 varies quadratically with the intermolecular overlap terms, thus

$$D_2^1(\text{IMD}, \text{BL}) = D_2^1(\infty, \text{BL}) \left[1 + \sum_{i,j=1}^2 \sum_{k \geq \ell > 2} K_{ikj\ell} S_{ik} S_{j\ell} + O(S^3) \right] \quad (4)$$

where $\{K_{ikj\ell}\}$ are positive constants in the cases we have examined. Thus, we should expect the minimum in C_{12} , and concomitantly the minimum in E , to be shifted in the direction which increases the intermolecular overlap terms. For example, when the intruder is an H atom approaching along the perpendicular bisector of the H_2 molecule, the optimum bond length should shrink. (A shrinkage of $.004 a_0$ has been observed for $IMD = 3.6 a_0$.)¹⁰ Similarly, we expect a shrinkage of the optimum bond length in rectangular H_4 . On the other hand, in the colinear approach of the intruder, the intermolecular overlap of the orbital localized closest to the intruder dominates in Eq. 4, and it determines the optimum H_2 bond length. Thus in the colinear encounter of an H atom or an H_2 molecule with the H_2 molecule, the optimum bond length should stretch. The stretching in colinear H_3 is well-known.¹¹ At smaller separations, the repulsive interactions become important in determining the optimum bond length of the molecule and the bond lengths may increase in either case.

A system may alter its spin coupling to minimize these deleterious contributions. The ability of the system to do this determines the barrier height of the surface, and, hence whether the collision will be reactive or nonreactive. Consider, for example, the reactive colinear collision of H_2 and H. At infinite separation, the H_2 orbitals are coupled into a singlet and the H atom orbital coupled to this singlet to produce a doublet; at the transition state, on the other hand, essentially,¹² the outer two orbitals are coupled into a triplet and the central orbital is coupled to this to produce a doublet. (That is the bonding of the central atom to the outer two is equivalent.)

There the attractive terms in the contragradience ($C_{12} + C_{23}$) have essentially the same dependence on internuclear distance as the H_2 molecule. The repulsive term, C_{13} , depends on $2R$ rather than on R , hence its maximum occurs inside the minimum in the attractive terms. Thus the minimum in C (and E) moves to larger internuclear distances, and the reactive collision increases the stretching we saw above.

The situation in the nonreactive collision is different, in such a collision, there exist more repulsive interactions than can be simultaneously minimized by a change in the spin-coupling. Thus the long-range trends observed above continue until C_{12} , is overwhelmed by the repulsive interactions. These terms are directly proportional to the intermolecular overlap; to minimize the energy here, the system must change in a manner which lowers the intermolecular overlap terms. This is exactly the opposite of the long-range effects, thus we expect the optimum BL as a function of IMD to exhibit an extremum for a nonreactive collision.

This minimum (a shrinkage of $.04 a_0$) is observed on the FOS at an IMD of $2.92 a_0$. The shapes of the FO and SCF surfaces are comparable except that the frozen surface is stretched out because of the crude nature of the wavefunction.

VI. COMPARISON WITH SEMIEMPIRICAL SURFACES

Rubenstein and Shavitt² have previously pointed out the rather disturbing discrepancy between semiempirical and theoretic determinations of the $H_2 + D_2$ reaction surface. Ab initio determinations¹⁻³

of this surface find a barrier height of some between 120 and 140 kcal · mole⁻¹ for the reaction; on the other hand, semiempirical¹³ approximations to the surface find a barrier height of 62 kcal · mole⁻¹. The discrepancy appears to arise from the basic assumption that the energies of the $^3\Sigma_u^+$ and $^1\Sigma_g^+$ states can be fitted to simple expressions involving effective Coulomb and exchange integrals which can then be used to represent the corresponding interactions in the H₂H₂ systems.

Making use of the dominance of the contragradience energy in chemical binding, a semiempirical scheme circumventing this assumption but using the exact H₂ energies to fit the contragradience quantities, has been developed.¹⁴ Using this scheme and the Kołos-Wolniewicz¹⁵ values for the $^1\Sigma_g^+$ and $^3\Sigma_u^+$ states of H₂, we find a barrier height of 117 kcal · mole⁻¹ for this reaction. While the virtually exact agreement between the theoretical and semi-empirical surfaces is, without a doubt, fortuitous, the qualitative agreement of the barriers indicates that it may be possible to obtain reliable energy surfaces using only the properties of diatomic systems.

SUMMARY

We have examined the orbitals and pair interactions over the energy surface for the collision of two H_2 molecules in a rectangular configuration using the contragradience energy. This technique allowed a detailed interpretation of the shapes of the surface using only the overlaps, the orbital shapes, and the spin-couplings. The FOS exhibited quite a different shape, and we found this was due to the presence of a large intermolecular repulsive term, which became greatly decreased upon allowing self-consistency.

The contraction of the bond lengths of the molecules, first noted by Conroy and Malli¹, was shown to arise naturally from consideration of the contragradience energy. It was shown not only to be real and reasonable, but possibly a quite common property of nonreactive collisions.

The contragradience concept appears to be quite powerful in understanding the detailed shapes of reaction surfaces. As was expected from earlier work, we were able to understand the shape of the surface in terms of the orbitals of the constituent molecules with only a moderate consideration of self-consistency effects.

ACKNOWLEDGEMENTS

CWW would like to thank Dr. H. B. Keller of Caltech's Applied Mathematics Division for several helpful discussions on numerical integration techniques, and Mr. Robert C. Ladner for the use of his quadratically convergent SOGI program.

REFERENCES

¹H. Conroy and G. Malli, J. Chem. Phys. 50, 5049 (1969). Conroy and Malli assume that the spin coupling is that of two singlets coupled into a singlet over the entire surface for rectangular H_4 . From the SOGI results (which allow both types of coupling) we see that the optimum spin coupling for the $^1B_{1g}$ state of the square is that of two triplets coupled into a singlet. This effect is negligible beyond 0.1 bohr⁶ from the square in the region considered. The only significant effect of this assumption appears to be that their optimum square occurs at too small a separation, they find this separation to be $2.22 a_0$ ⁴ whereas Rubenstein and Shavitt³ find it to be $2.47 a_0$, and we obtain $2.48 a_0$ here. Of course no such problem would arise if they had been able to use a complete basis set and include all possible excited configurations. [See W. A. Goddard III, Phys. Rev. 157, 73 (1968); the exact wavefunction can be written in terms of any specified spin-coupling if no restrictions are made in the spatial part of the wavefunction.]

²C. W. Wilson, Jr., and W. A. Goddard, III, J. Chem. Phys. 51, 716 (1969).

³M. Rubenstein and I. Shavitt, J. Chem. Phys. 51, 2014 (1969).

⁴Atomic units are used throughout his work. The unit of energy is the hartree = $627.51 \text{ kcal/mole}^{-1} = 27.211 \text{ eV}$, the unit of length is the bohr = 0.52917 \AA .

⁵The authors wish to thank Mr. Robert C. Ladner for helping in choosing this basis set, and Mr. David L. Huestis for the use of his version of MOSES, the Murray Geller Integral Program, with which the integrals were computed.

⁶R. C. Ladner and W. A. Goddard, III, J. Chem. Phys. 51, 1073 (1969).

⁷(a) C. W. Wilson, Jr., and W. A. Goddard, III, Chem. Phys. Lett., 5, 45 (1970); (b) Bull. Am. Phys. Soc. 14, 1192 (1969); (c) J. Chem. Phys., to be published.

⁸W. A. Goddard, III, Phys. Rev. 157, 73, 81 (1967).

⁹For the SCF wavefunctions, the contragradience energy for each pair of orbitals was calculated using a mixed Gauss-Legendre, Gauss-Laguerre three-dimensional numerical integration scheme using 31104 points. Those for the FO wavefunction were done analytically using 1s STO's.

¹⁰R. C. Ladner, C. W. Wilson, Jr. and W. A. Goddard, III, unpublished work.

¹¹See, for example, I. Shavitt, R. Minn, R. Stevens, and M. Karplus, J. Chem. Phys. 49, 1700 (1969).

¹²The actual solution of the SOGI equations produced delocalized orbitals [R. C. Ladner and W. A. Goddard, III, Int. J. Quant. Chem. 3S, 63 (1969)] which are, very nearly, linear combinations of our localized orbitals, the energy difference is 0.002 h at the transition state. Thus it would appear reasonable to discuss the surface in terms of these localized functions.

¹³(a) H. Eyring, J. Amer. Chem. Soc. 53, 2537 (1931); (b) S. W. Benson and G. R. Hangen, J. Amer. Chem. Soc. 87, 4036 (1965); S. W. Benson and A. N. Bose, J. Chem. Phys. 39, 3463 (1963); (c) K. Morokuma, L. Pedersen, and M. Karplus, J. Amer. Chem. Soc.

89, 5064 (1967); and R. B. Abrams, J. C. Patel, and F. O. Ellison, J. Chem. Phys. 49, 450 (1968).

¹⁴C. W. Wilson, Jr., to be published.

¹⁵W. Kołos and L. Wolniewicz, J. Chem. Phys. 43, 2429 (1965).

FIGURE CAPTIONS

- Fig. 1 The energy surface⁴ for rectangular H_4 . All quantities are in atomic units.
- a. The SOGI surface. The minimum energy square occurs at $2.48 a_0$ with an energy of $-2.0721 h$.
 - b. The frozen surface. The minimum square occurs at $2.67 a_0$ with an energy of $-2.0539 h$.
- Fig. 2a A SOGI orbital for rectangular H_4 , $IMD = 3.6$ and $BL = 1.4$. The other three orbitals are symmetrically related to this one by the various σ_v operations. (The contour spacing is 0.05, the nodal line is dashed.)
- Fig. 2b A SOGI orbital for rectangular H_4 , $IMD = 2.4$ and $BL = 1.4$. The symmetry of the other orbitals remains as in Fig. 2a. (The contour spacing is 0.05, the nodal line is dashed.)
- Fig. 2c A SOGI orbital for rectangular H_4 nearing the square, $IMD = 2.2$ and $BL = 2.0$. The symmetry of the other orbitals remains as in Fig. 2a. (The contour spacing is 0.05, the nodal line is dashed.)
- Fig. 3 The contragradience energy C , and the total energy E as a function of BL for $IMD = 2.6 a_0$.
- Fig. 4 The total contragradience energy for rectangular H_4 .
- a. The SOGI surface.
 - b. The frozen surface.

Fig. 5 The contribution to the contragradiance energy due to the pair (13) localized along the diagonal of the rectangle in rectangular H_4 .

- a. The SOGI surface.
- b. The frozen surface.

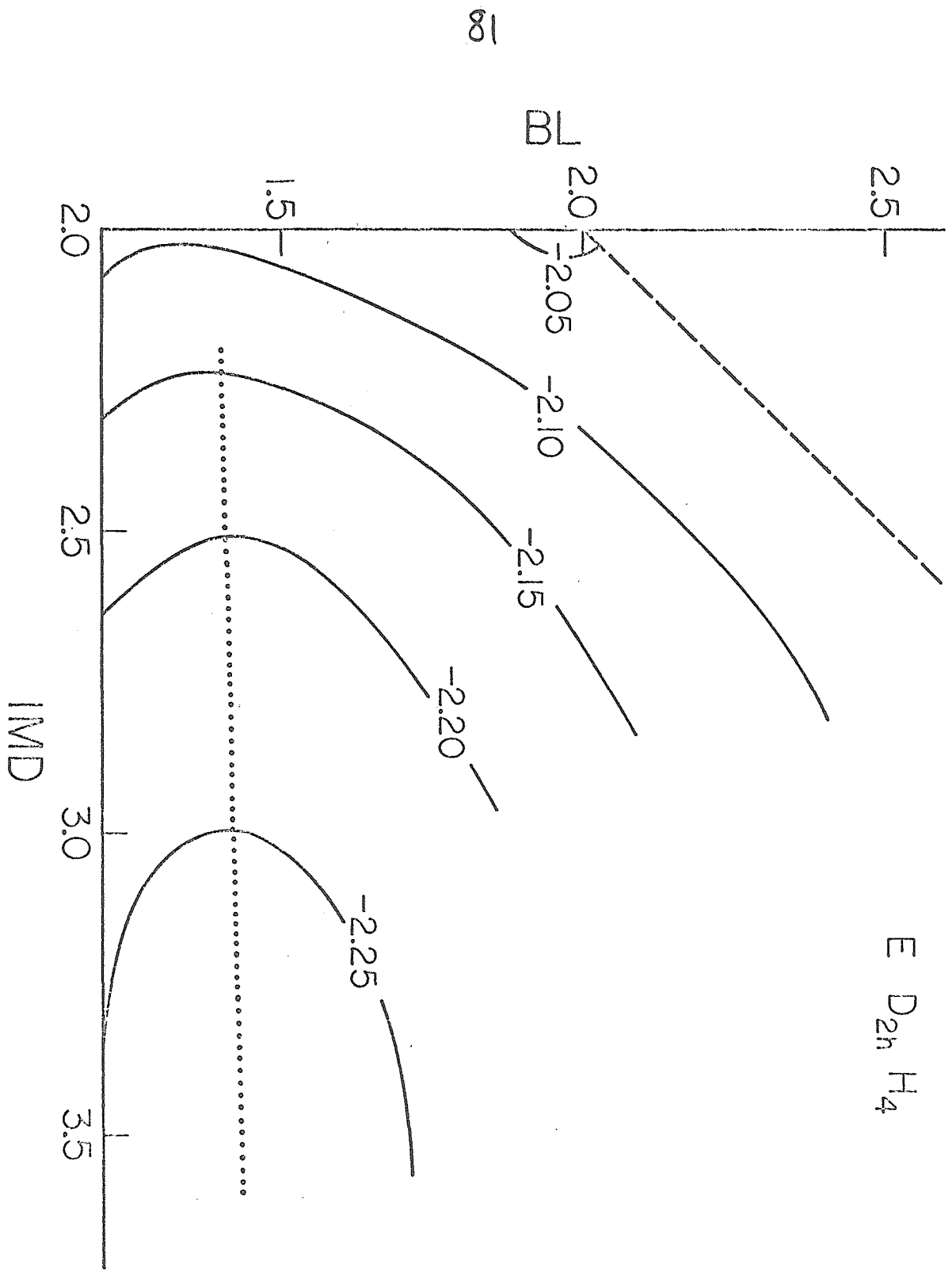
Fig. 6 The contribution to the contragradiance energy due to the pair (14) localized along the long side of the rectangle in rectangular H_4 .

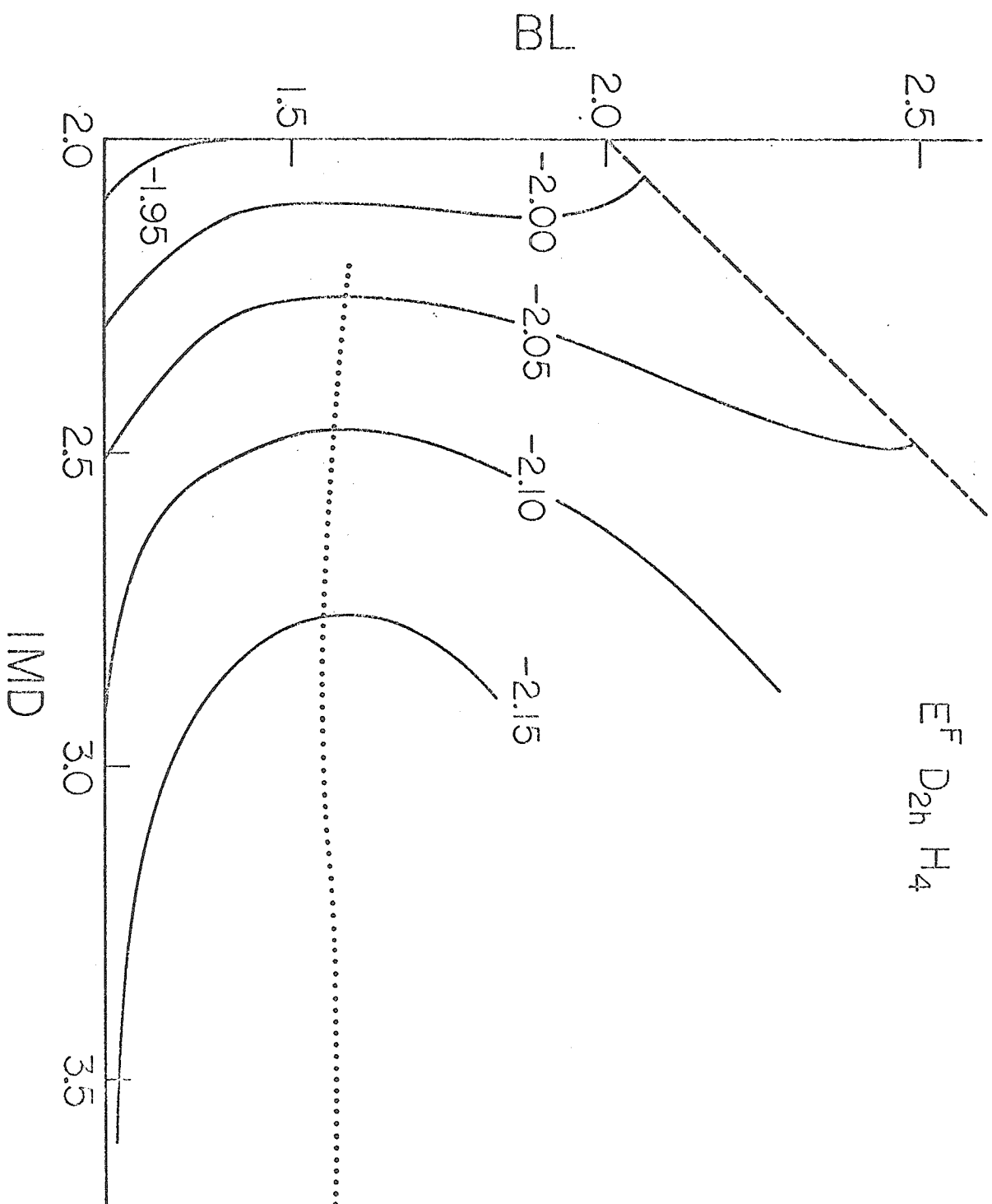
- a. The SOGI surface.
- b. The frozen surface.

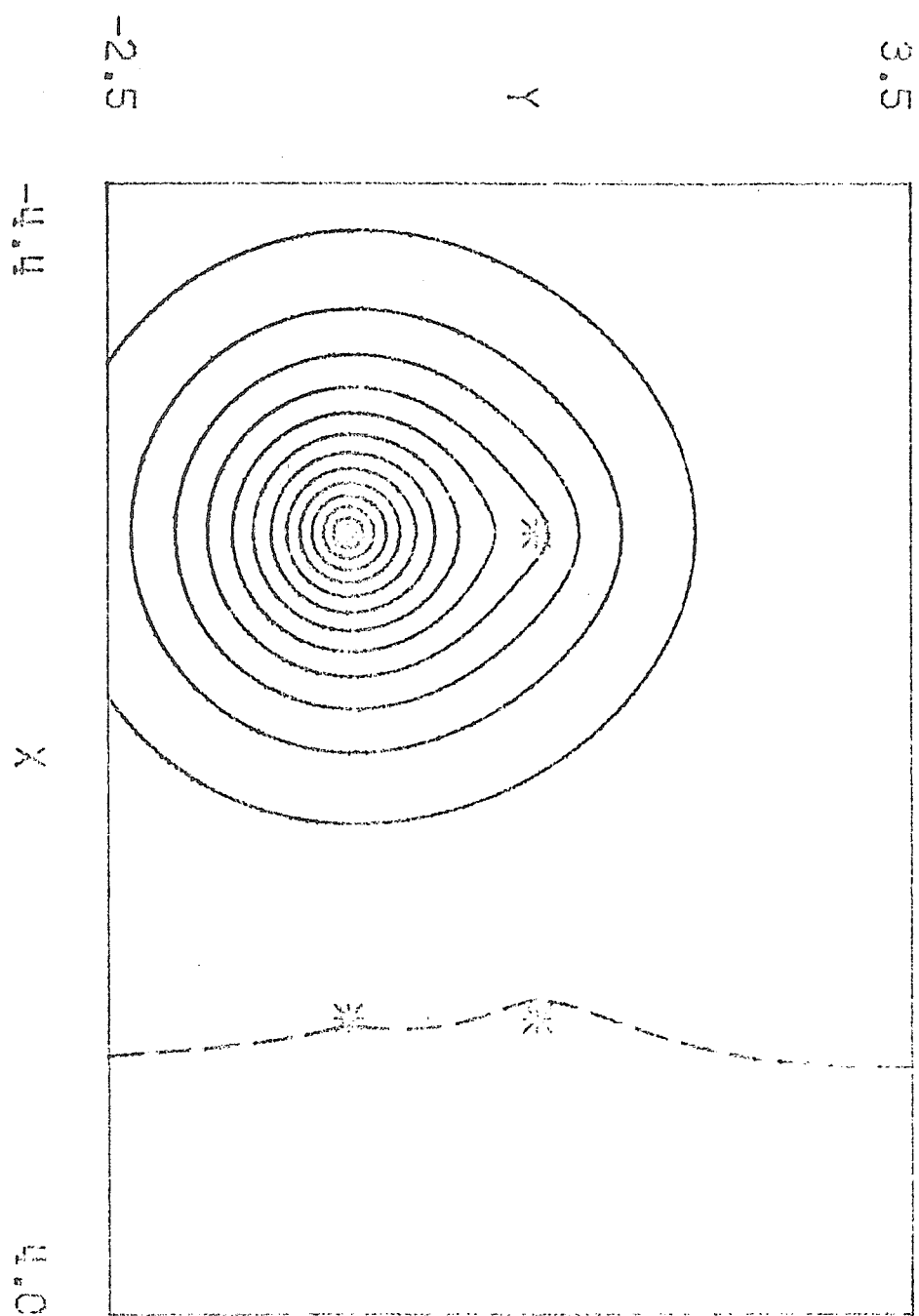
Fig. 7 The contribution to the contragradiance energy due to the pair (12) localized along the short side of the rectangle in rectangular H_4 .

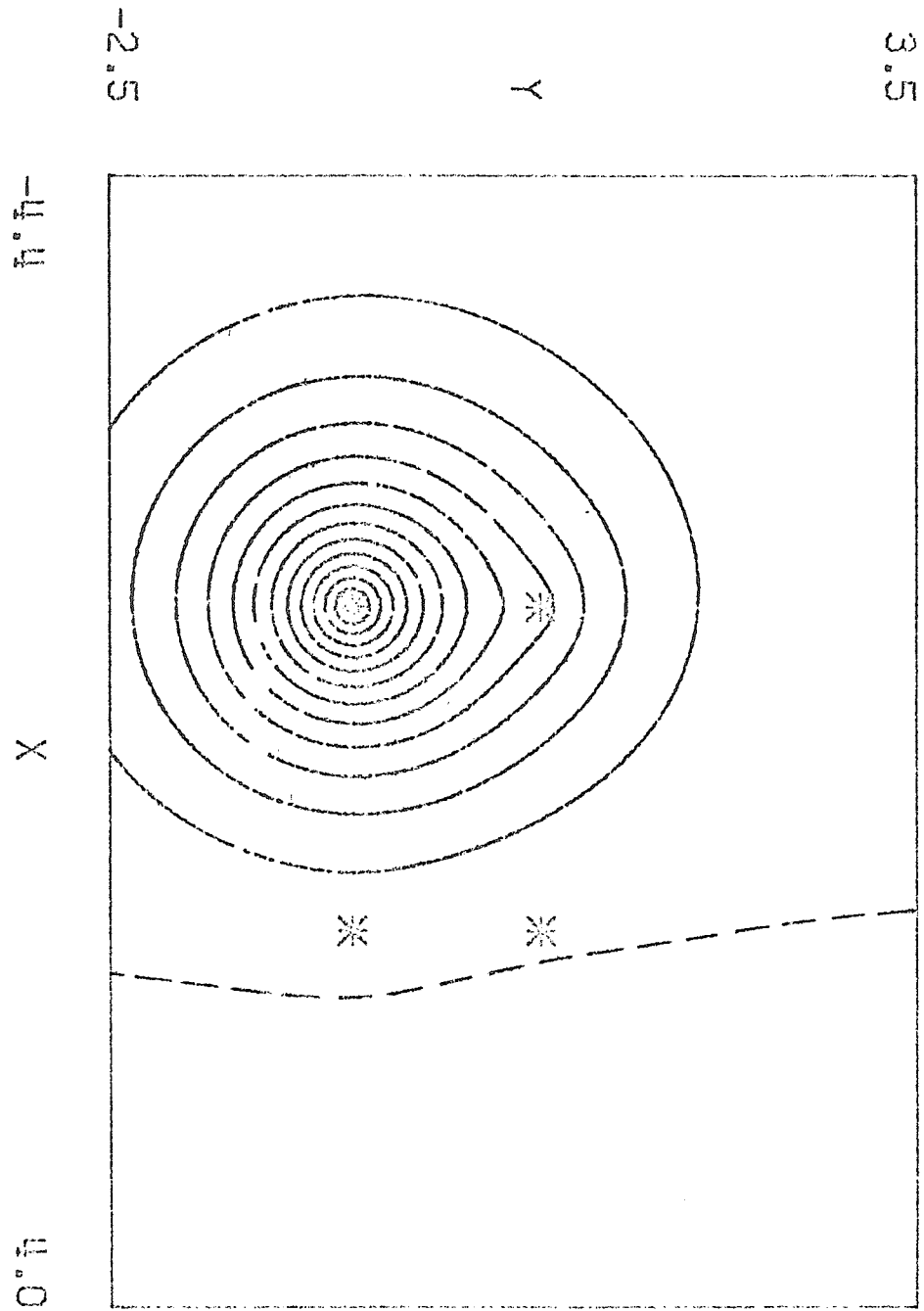
- a. The SOGI surface.
- b. The frozen surface.

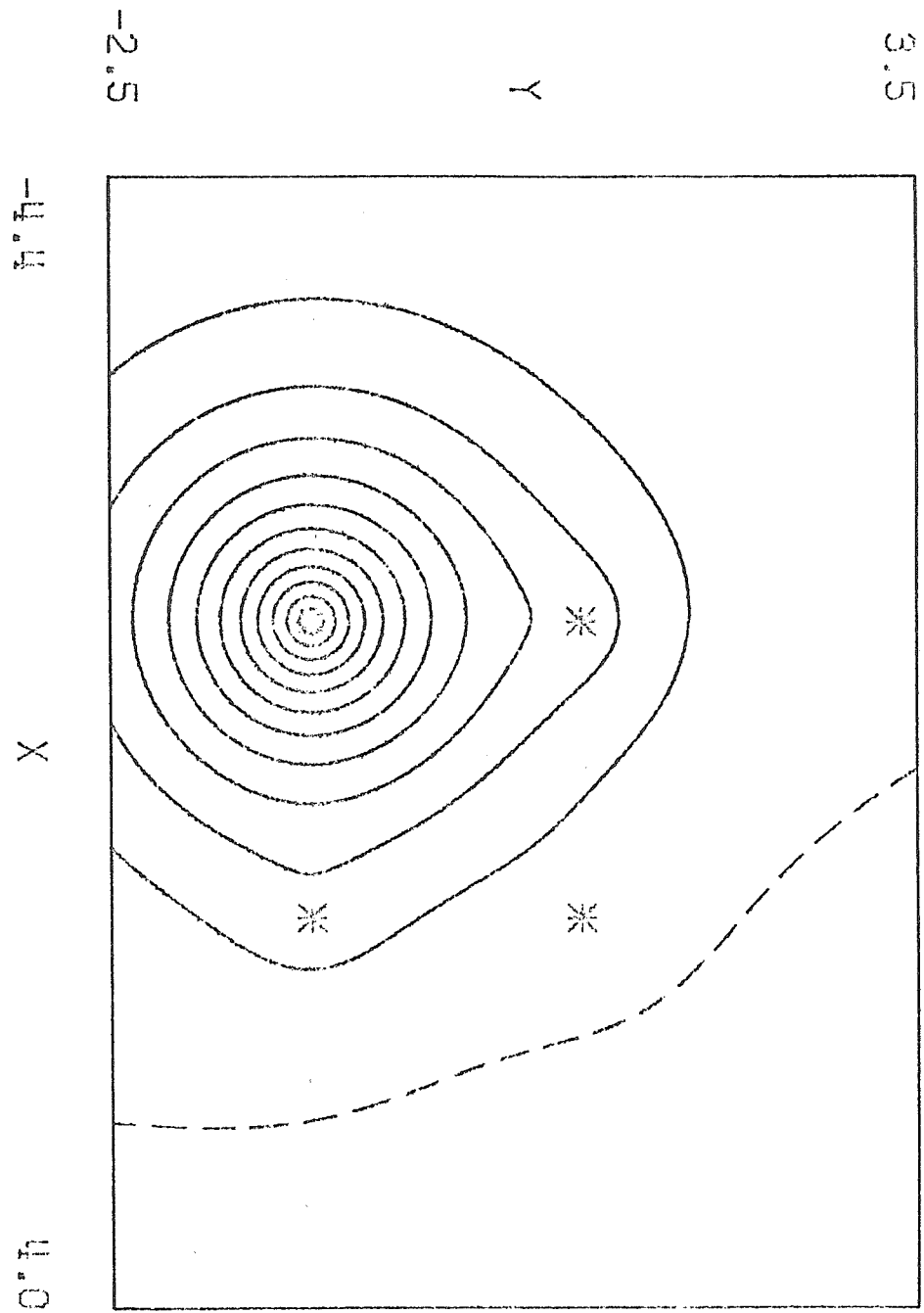
$E_{D_{2n}H_4}$

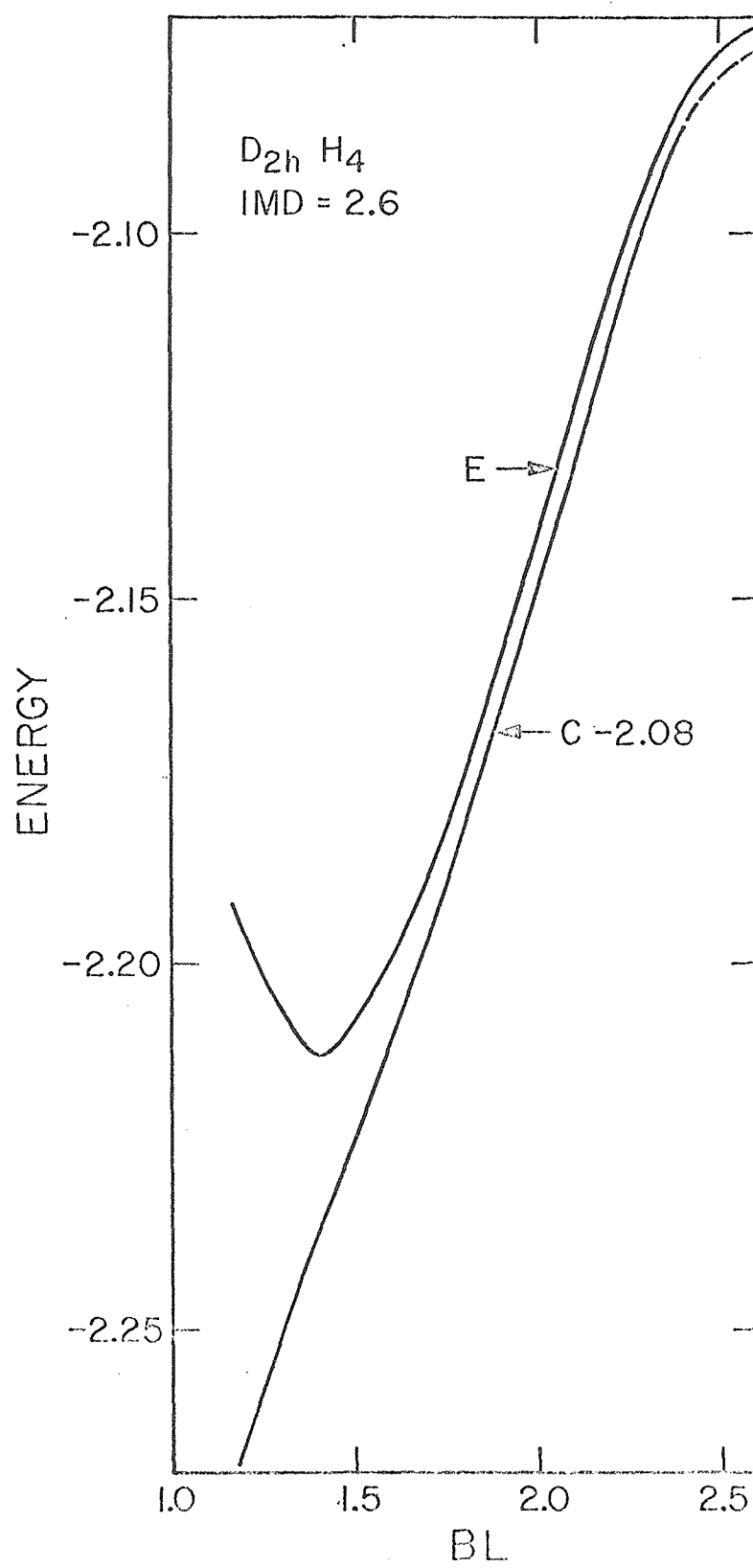


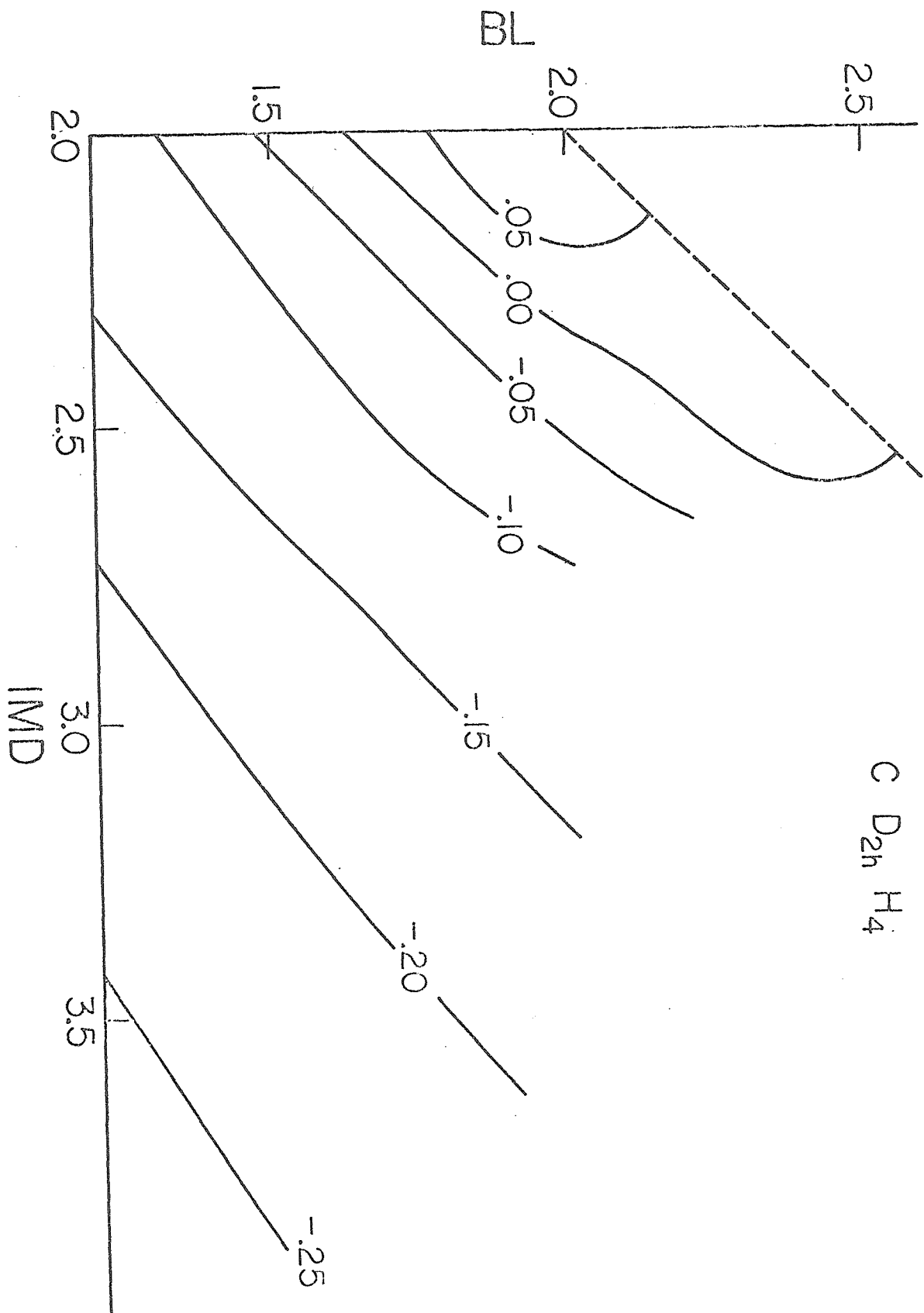


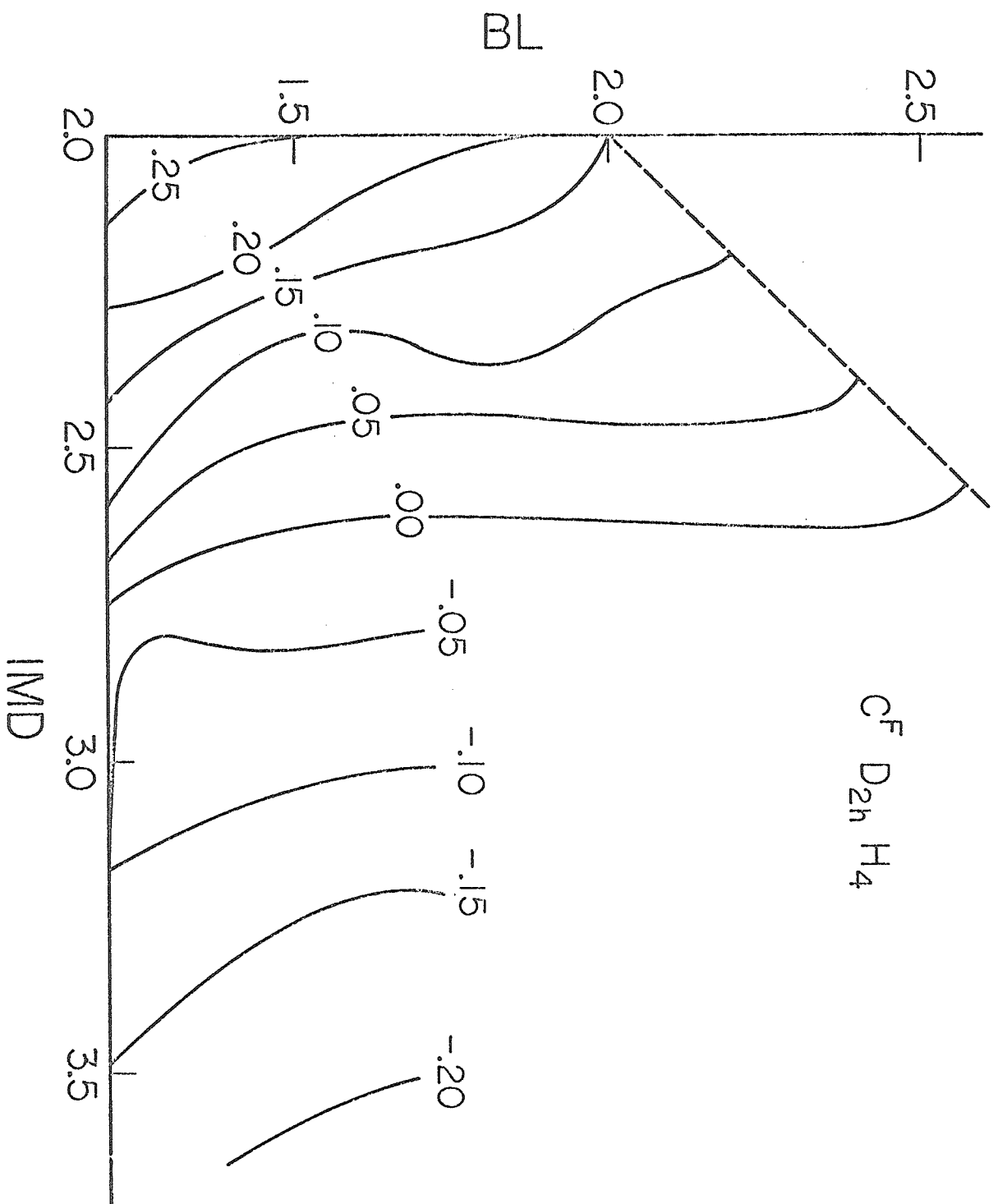


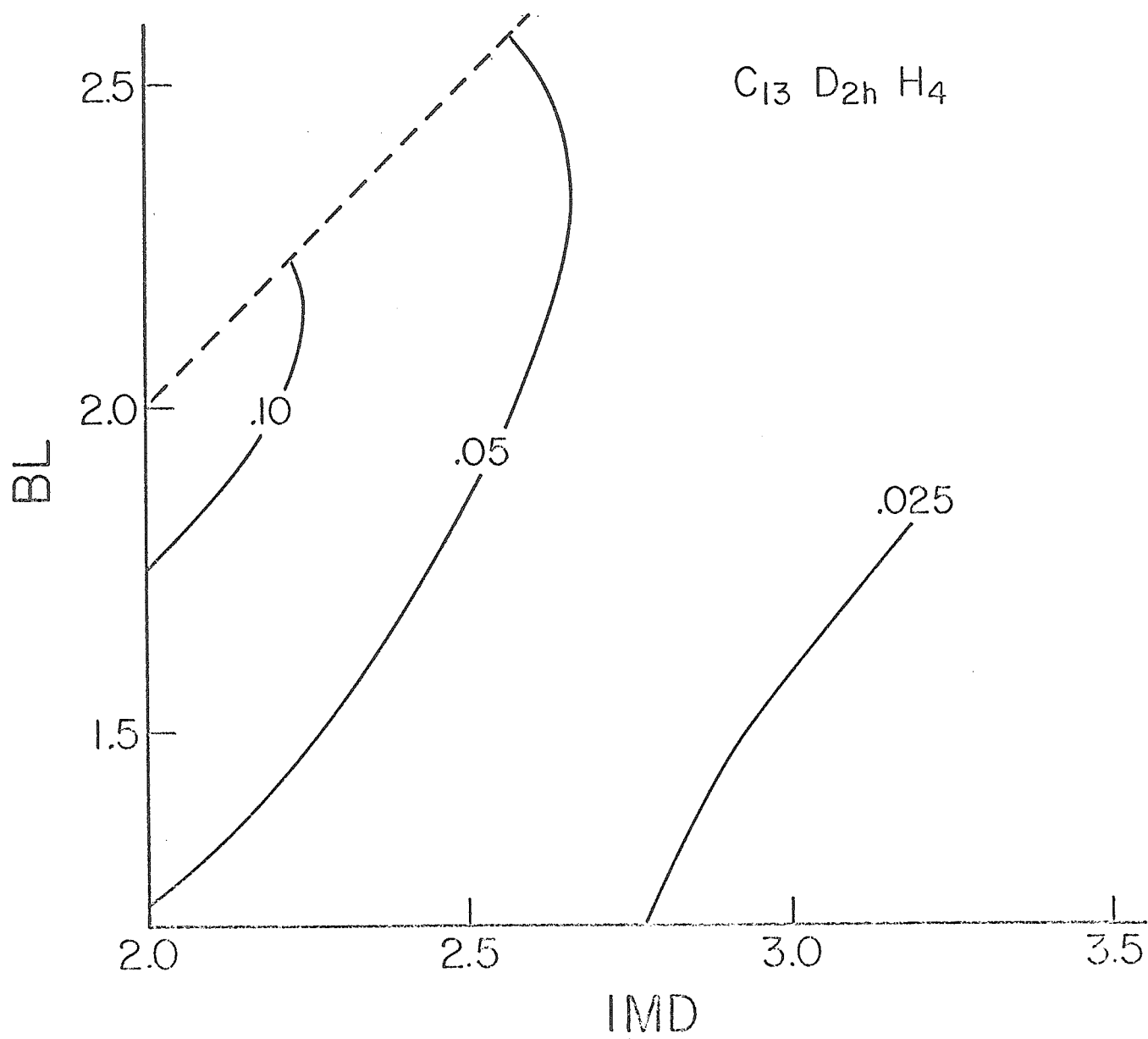




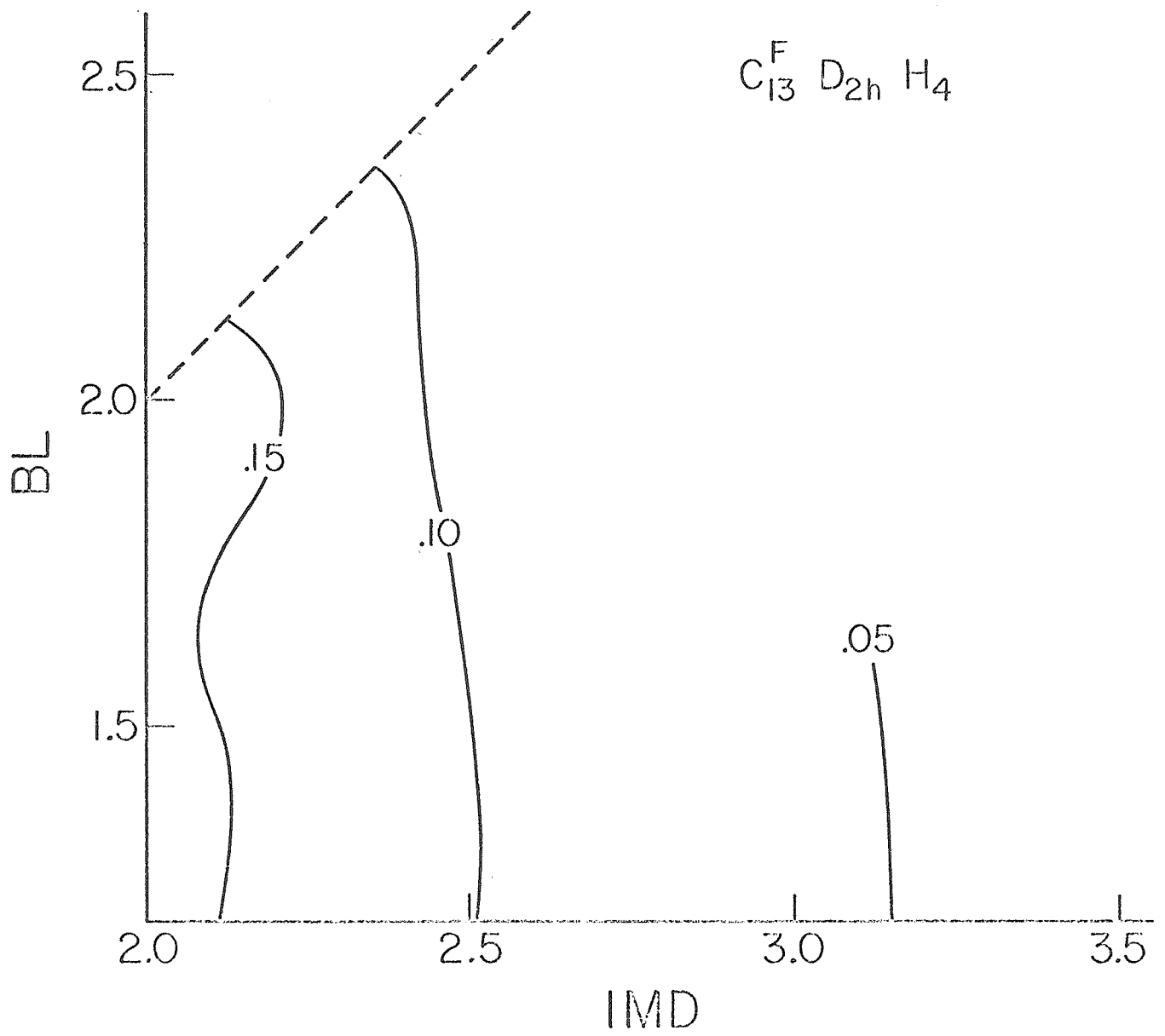




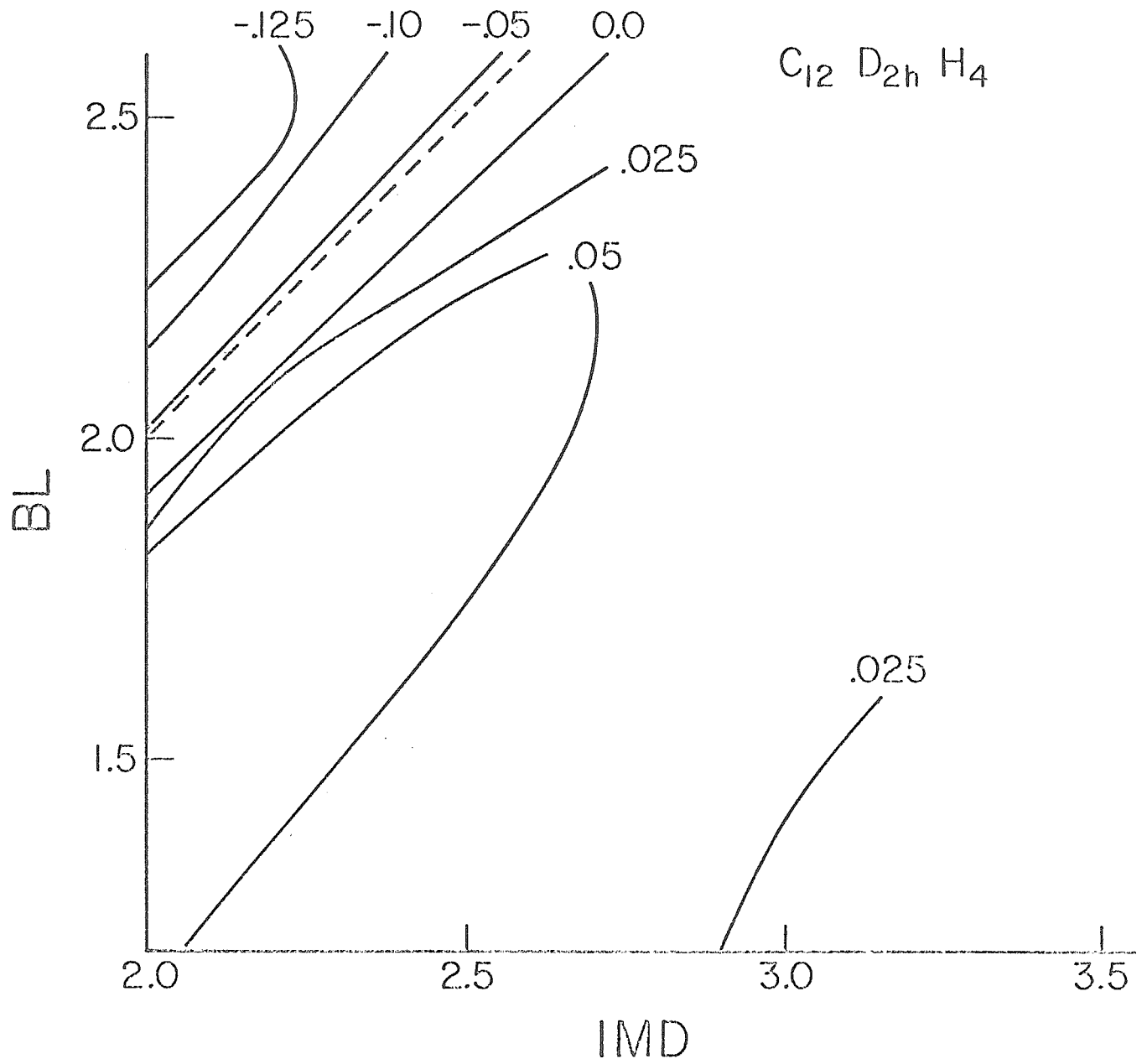


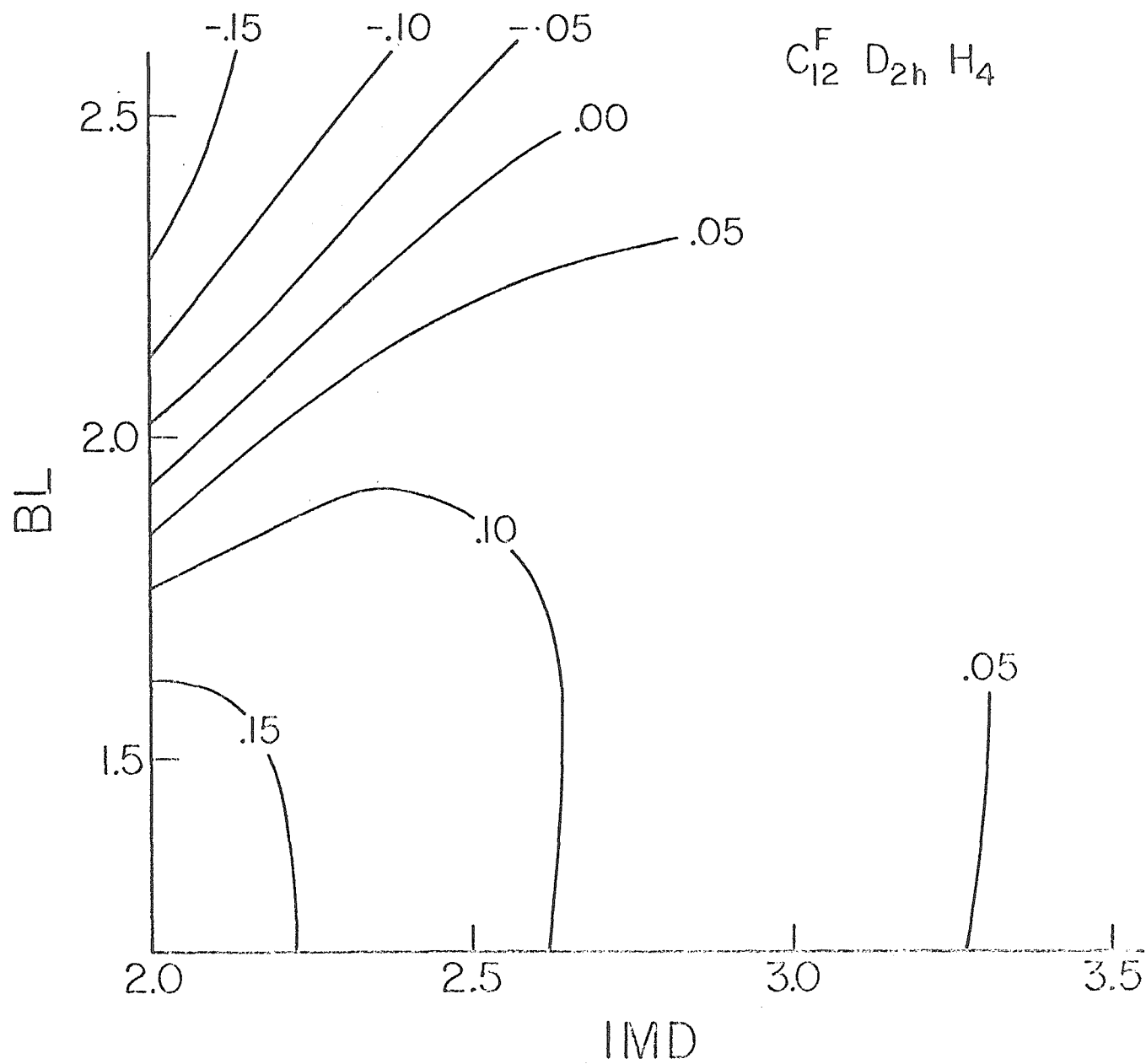


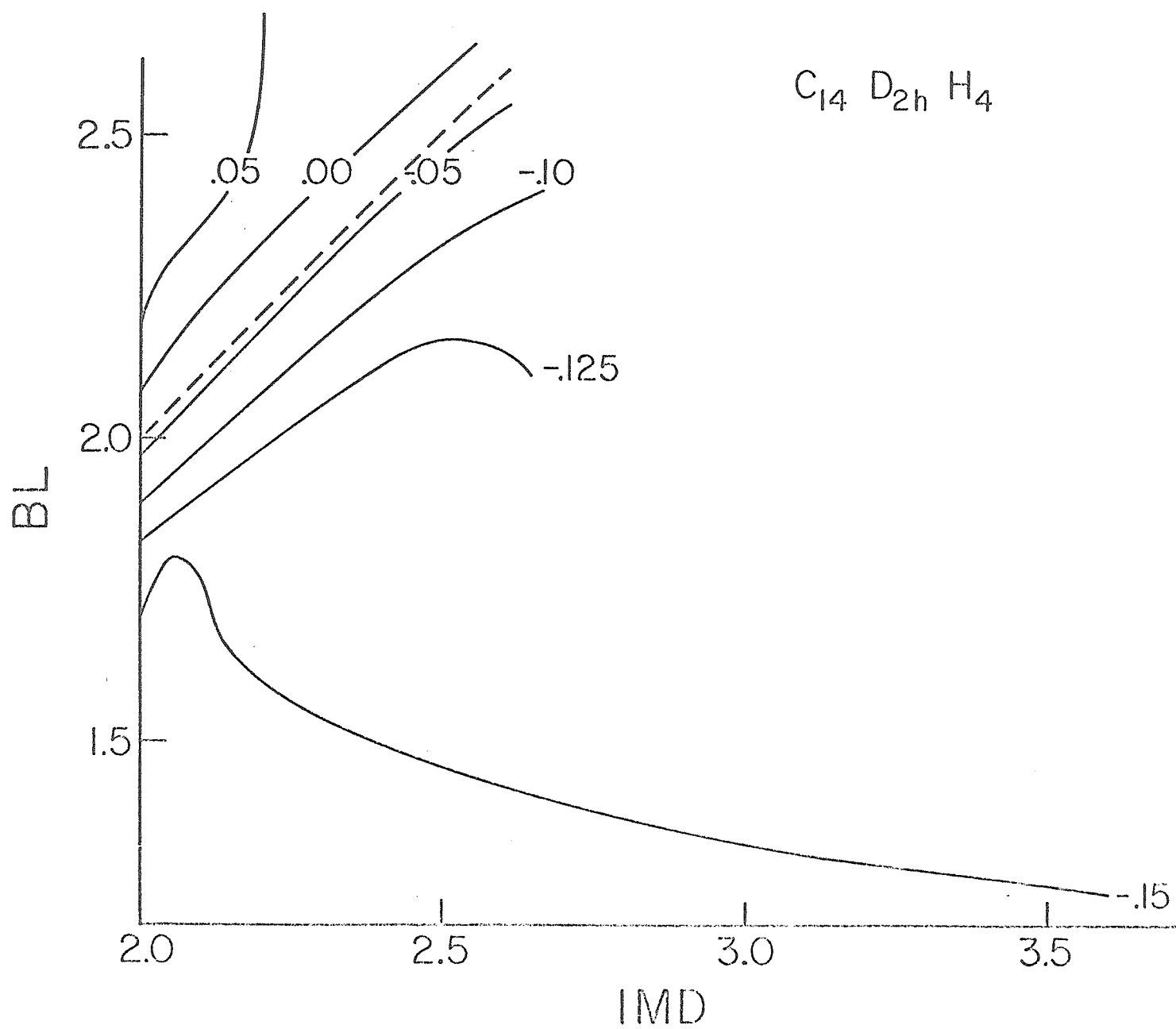
90

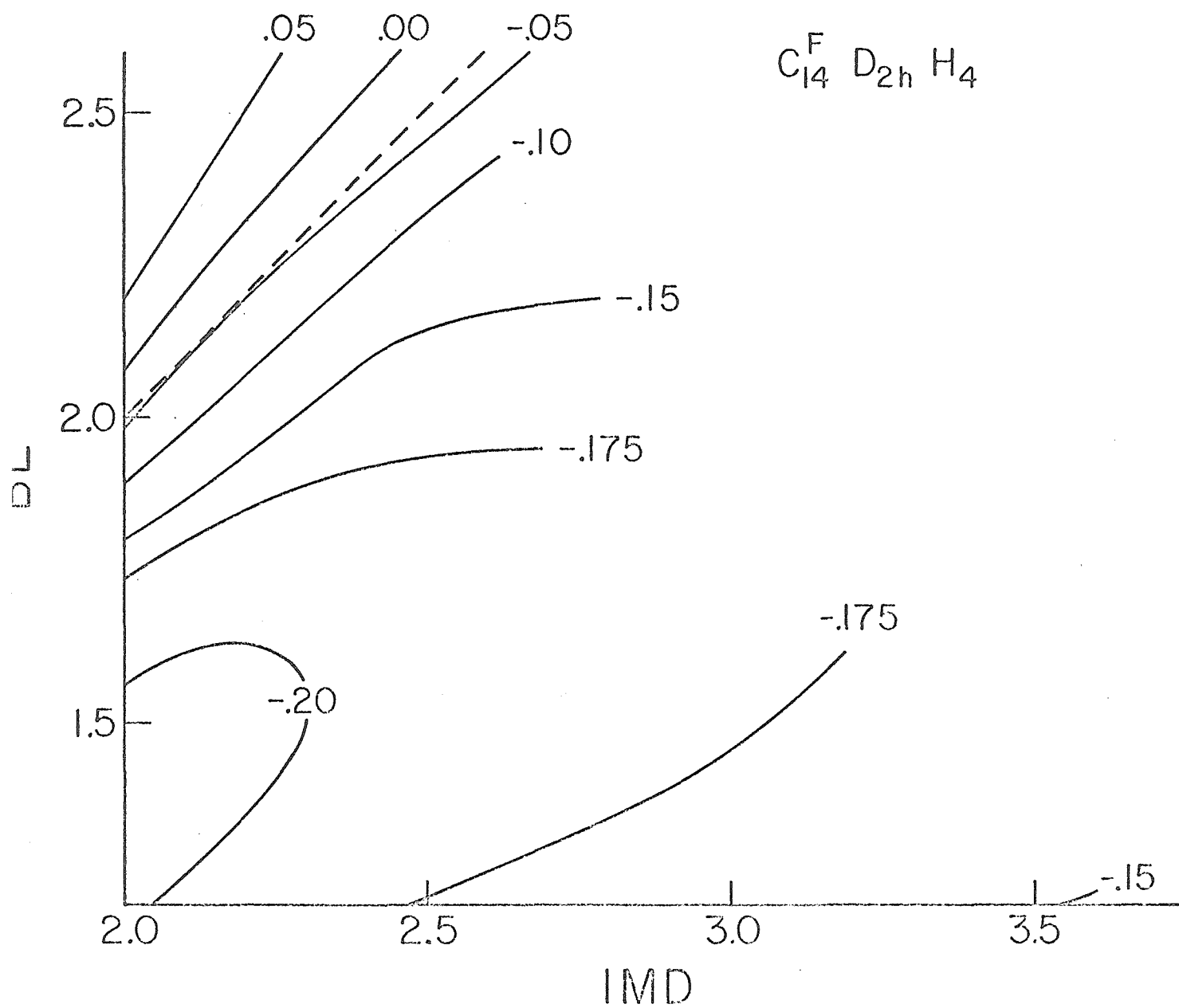


91.









A P P E N D I X B

TABLE I

A tabulation of useful quantities from minimum basis set G1 calculations on the ground $^1\Sigma_g^+$ state of H_2 --Self-consistent Calculations

R	ζ	E	S	C
1.0	1.306722	-1.093664		
1.1	1.276874	-1.120250		
1.2	1.249324	-1.136172		
1.3	1.223922	-1.144617		
1.4	1.200525	-1.147776	.796857	-.142662
1.43042	1.193785	-1.147937		
1.5	1.179000	-1.147189		
1.6	1.159222	-1.143956	.762062	-.135182
1.7	1.141076	-1.138876		
1.8	1.124457	-1.132535	.724464	-.127996
1.9	1.109270	-1.125370		
2.0	1.095425	-1.117707	.684346	-.120863
2.2	1.071443	-1.101814	.641935	-.113597
2.4	1.051925	-1.086191	.597578	-.106012
2.6	1.036348	-1.071598	.551765	-.097984
2.8	1.024222	-1.058454	.505124	-.089464
3.0	1.015075	-1.046953	.458401	-.080502
3.2	1.008435	-1.037143		
3.4	1.003838	-1.028968	.367984	-.061961
3.6	1.000841	-1.022300		
3.8	.999040	-1.016968		
4.0	.998085	-1.012780		
4.2	.997695	-1.009541	.218053	-.029754
4.4	.997658	-1.007070		
4.6	.997821	-1.005205	.163299	-.018902
4.8	.998080	-1.003812		
5.0	.998370	-1.002779		
5.5	.999029	-1.001241	.082547	-.005968
6.0	.999475	-1.000544	.055928	-.002988
6.5	.999734	-1.000235		
7.0	.999871	-1.000101	.025328	-.006984
7.5	.999939	-1.000042		
8.0	.999972	-1.000018	.011297	-.001525

T A B L E II

A tabulation of useful quantities from minimum basis set G1 calculations on the ground $^1\Sigma_g^+$ state of H_2 --Frozen Calculations

R	E	S	C
1.0	-.996424	.858385	-.121210
1.1	-1.041179	.833287	-.132055
1.2	-1.071987	.807200	-.141319
1.3	-1.092540	.780349	-.148922
1.4	-1.105473	.752942	-.154834
1.4304242	-1.108206		-.156298
1.5	-1.112717	.725173	-.159004
1.6	-1.115709	.697215	-.161656
1.7	-1.115540	.669230	-.162686
1.8	-1.113049	.641359	-.162253
1.9	-1.108883	.613729	-.160474
2.0	-1.103551	.586452	-.157484
2.2	-1.090888	.533332	-.148453
2.4	-1.077306	.482619	-.136362
2.6	-1.064144	.434748	-.122389
2.8	-1.052149	.389995	-.107589
3.0	-1.041674	.348509	-.092832
3.2	-1.032816	.310336	-.078770
3.4	-1.025514	.275440	-.065846
3.6	-1.019619	.243727	-.054312
3.8	-1.014942	.215057	-.044206
4.0	-1.011285	.189261	-.035696
4.2	-1.008461	.166150	-.028513
4.4	-1.006303	.145527	-.022581
4.6	-1.004668	.127189	-.017748
4.8	-1.003440	.110936	-.013852
5.0	-1.002524	.096577	-.010745
5.5	-1.001145	.067772	-.005560
6.0	-1.000509	.047096	-.002725
6.5	-1.000222	.032449	-.001572
7.0	-1.000096	.022189	-.000800
7.5	-1.000041	.015071	-.000312
8.0	-1.000017	.010175	-.000145